

Elements of Active Vibration Control for Rotating Machinery

Heinz Ulbrich
Lewis Research Center
Cleveland, Ohio

May 1990

(NASA-TM-102368) ELEMENTS OF ACTIVE
VIBRATION CONTROL FOR ROTATING MACHINERY
(NASA) 50 p
CSCL 13B

N90-22703

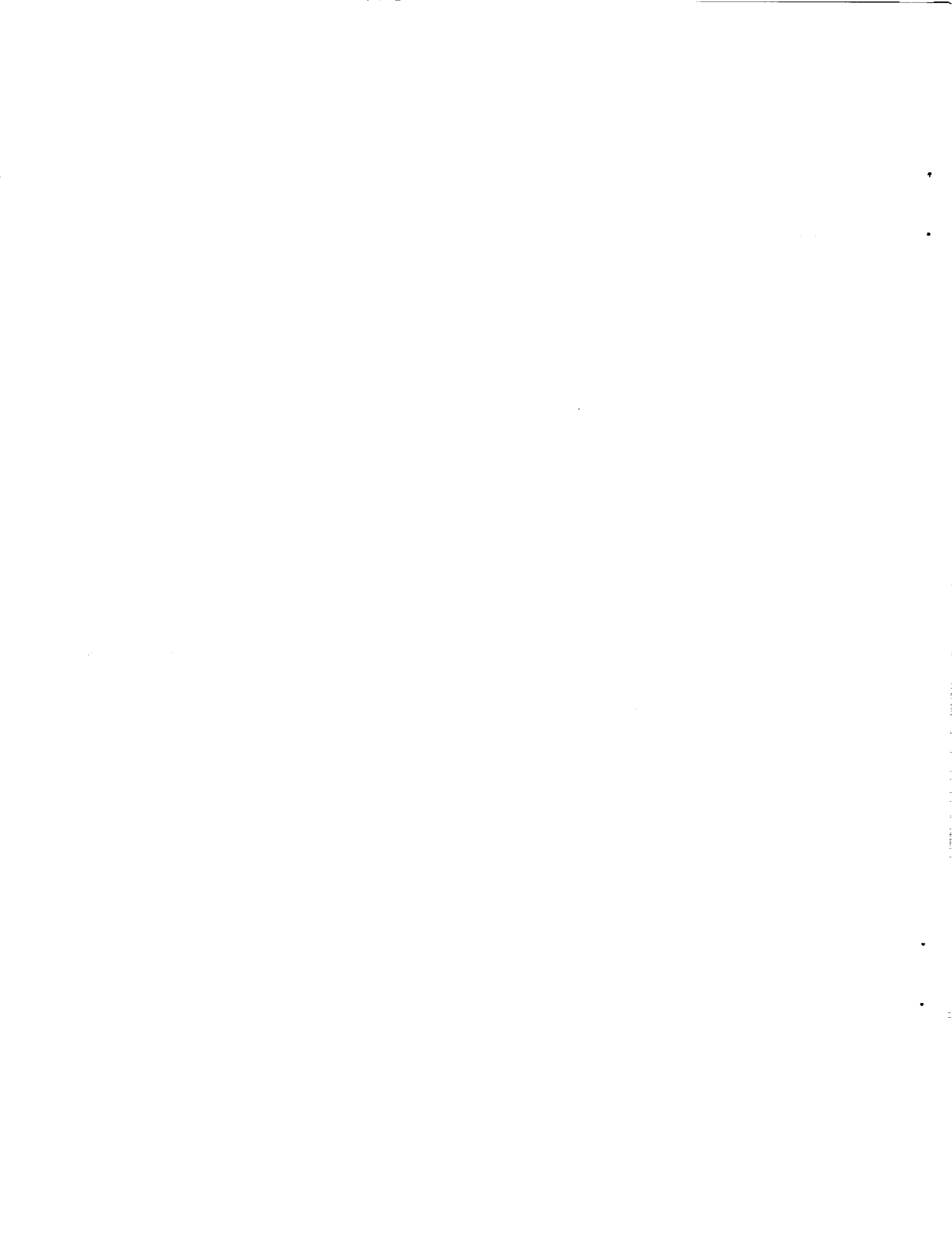
Unclas
G3/31 0286255

NASA



CONTENTS

	Page
SUMMARY	1
INTRODUCTION	1
ACTUATORS, MODELS, AND TRANSFER CHARACTERISTICS	2
Magnetic Actuators	2
Active magnetic bearing	2
Electromagnetic actuator	3
Active chamber system	3
MODELING OF ACTIVELY CONTROLLED ROTOR SYSTEMS	5
Modeling of Rotor Systems to be Controlled	5
Modeling of Complete System	10
Inclusion of electromagnetic actuators	11
Inclusion of active chamber system	12
Discussion of Several Cases	14
Proportional derivative (PD) controller	14
Proportional derivative-acceleration (PDA) controller	14
Proportional integral derivative-acceleration (PIDA) controller	15
CONTROLLABILITY, OBSERVABILITY, AND SPILLOVER	15
Controllability and Observability	15
Spillover	16
CONTROL CONCEPTS AND CONTROLLER OPTIMIZATION	19
State Feedback Control	20
Output Feedback Control	21
EXAMPLES AND RESULTS	22
Magnetic Suspension of an Epitaxy Centrifuge	22
Equations of motion and state	22
Radial forces acting on the rotor	23
Control of an Elastic Rotor	26
State feedback control (Riccati controller)	27
Output feedback control	29
CONCLUDING REMARKS	30
APPENDIX - SYMBOLS	31
REFERENCES	36



ELEMENTS OF ACTIVE VIBRATION CONTROL FOR ROTATING MACHINERY

Heinz Ulbrich*
National Aeronautics and Space Administration
Lewis Research Center
Cleveland, Ohio 44135

SUMMARY

Demands for higher frequencies, improved reliability, reduced noise, and increased longevity, along with safety concerns, require an effectively controlled rotor dynamics system. The desired requirements are often not met by using only passive damping elements; further improvements can be achieved only with the aid of active control. Showing how to construct a controller and how to apply active control on rotating machinery is the intent of this report.

Different types of actuator concepts and their models are discussed. The modeling of rotor systems is given in such a way that inclusion of active elements can easily be achieved. The chosen modeling procedure, which is both physically clear and handy for computer-oriented representation, permits both the consideration of all mass and gyroscopic effects and a modular construction of the system. The meaning of controllability, observability, and spillover, with regard to actively controlled systems, and a method to check on the system properties are discussed. A short introduction about control concepts and the optimization of the controller is given. In the last section several real applications demonstrate the design and application of active vibration control.

INTRODUCTION

In the growing field of rotor system dynamics control, many different methods have been applied. The methods that have been proposed for rigid and flexible rotors differ in control concepts (refs. 1 to 8). The type of controller that is most effective depends on the objectives. The controller normally makes use of four elements:

- (1) Displacement (proportional) feedback (P part), which allows one to change the stiffness of the system or, in other words, to shift the eigenfrequencies in the desired manner
- (2) Velocity (derivative) feedback (D part), which permits one to increase the system damping to (a) improve the stability of the system, (b) stabilize unstable modes of the system, or (c) reduce resonance amplitudes that can occur when rotors pass through critical speeds
- (3) Acceleration feedback (A part), which can be used to eliminate or reduce the influence of the mass or inertia (e.g., improving the controllability in relation to applying active forces via the bearing housings (ref. 4), or compensating for the influence of fluid inertia in relation to hydraulic actuators (ref. 2))

*National Research Council - NASA Research Associate at Lewis Research Center.

- (4) Integral feedback (I part), which is necessary for holding a rotor position very precisely (no radial displacement) at a given location, or for adjusting bearings to minimize rotor stress (minimum stress is achieved by changing the features of the bearing or the foundation of the bearing supports).

The type of feedback control that is chosen will depend on one's objectives and the system itself.

To realize active control techniques for improving the dynamic behavior of rotor systems, the following are required: (1) suitable actuators and knowledge of their transfer characteristics; (2) modeling of the complete system (including the active components); (3) choosing locations for actuators and sensors (affects controllability, observability, and spillover effects); and (4) having problem-adapted control methods for hardware as well as software.

The key to successful active vibration control in rotor systems (i.e., systems with rotating machinery) lies in the availability of suitable actuators. Some types of actuator that have been applied in industry or in the test stage in the laboratory will be introduced in this report.

ACTUATORS, MODELS, AND TRANSFER CHARACTERISTICS

In general, there are two different ways to apply control forces on rotating shafts in turbine engines, power generators, gearboxes, machine tools, and such. The forces can act directly on the rotor or they may be applied via the bearing housings. For practical applications the following characteristics are very important:

- (1) Actuators should not only be compact but also be capable of generating large forces.
- (2) The amplitude range of the actuator should be at least as high as the vibration amplitudes that have to be influenced.
- (3) The frequency range of the actuator (bandwidth) that can be obtained will determine the applications. This means the design strategies for the actuators will have to focus to a high degree on the actuator dynamics. In this section three different types of actuators will be introduced and their mathematical descriptions of the transfer characteristic will be given.

Magnetic Actuators

Magnetic actuators can be divided into two types: magnetic bearings, which act directly on the rotor without contact (refs. 1, 2, 9, and 10), and electromagnetic actuators, which apply forces to the rotor indirectly via the bearings (refs. 3, 5, and 11 to 13).

Active magnetic bearing. - A typical assembly of electromagnets (EMX1, EMX2, EMY1, EMY2) is represented in figure 1. It is noteworthy that with this arrangement of the magnets, radial movement of the rotor in the y-direction

causes no change in the total air gap of the magnetic circuits in the x-direction (comparative effect). This is necessary for decoupling the forces of the bearing between the x- and y-directions. The differential arrangement of the electromagnets leads to a linear input/output characteristic between the forces acting directly on the rotor and the control voltages input to the power amplifiers. The power amplifiers have to work, in this case, as current sources. This relationship between the input voltages u_x and u_y and the resulting forces F_x and F_y is given by

$$\begin{bmatrix} F_x \\ F_y \end{bmatrix} = \begin{bmatrix} k_u & 0 \\ 0 & k_u \end{bmatrix} \begin{bmatrix} u_x \\ u_y \end{bmatrix} + \begin{bmatrix} k & 0 \\ 0 & k \end{bmatrix} \begin{bmatrix} x \\ y \end{bmatrix} \quad (1)$$

where k_u represents the force-voltage factor; k , the force-displacement factor (negative of stiffness); and x and y , the radial displacements of the rotor in the respective directions. Figure 2 shows a schematic of a controlled-orbit magnetic bearing test rig to determine k_u , k , and the frequency characteristic. The rotor is fixed by ball bearings and its position is measured by built-in noncontacting displacement transducers. Forces on the rotor are simultaneously determined in the x- and y-directions by quartz load washers. In order to decouple the forces into the two measurement directions, special axial linear roller guides are used. This means the quartz load washers are attached to the foundation in such a way that a force in the x-direction (and similarly, in the y-direction) does not influence the force signal in the y-direction (x-direction); see references 10 and 14.

Electromagnetic actuator. - An electromagnetic actuator capable of applying forces to the rotor indirectly via the bearing housing is shown in figure 3. The scheme shows a cross section of this active element, consisting mainly of two annular electromagnets acting in differential principle on a pull disk. If the power amplifiers work as current sources, the input/output characteristic is described by the same equation as that for the magnetic bearing (eq. (2)). The transfer characteristic of the actuator is shown in figure 4(a). The control force is displayed as a function of the control current. The deviation of the pull disk from its neutral position functions as a parameter. Figure 4(b) gives an impression of the frequency characteristic. Results show that the actuator can be modeled as a proportional transfer element at up to 300 Hz (cutoff frequency). These results could be achieved only by using special guided roller bearings to reduce friction in the guides of the connecting rod. Magnetic bearings and electromagnetic actuators require a relatively large amount of space in relation to the magnitude of attainable forces; this drawback may be avoided by the use of hydraulically controlled chambers.

Active chamber system. - The compact active chamber system, shown in figure 5, is capable of generating very large forces and can thereby influence even large turbines weighing several tons (see ref. 15). The actuator device consists mainly of four cylindrical chambers arranged in a circle around the outer bearing housing. Each chamber is sealed at the top and bottom by an elastic membrane. In order to decouple the forces in the x- and y-directions, the bearing housing is supported against the membrane system by linear roller guides. The influence of friction is thereby reduced as well. Alternative methods of support result from design variations. One variation supports the bearing via elastic rods - another, simply by chambers designed in such a way that they have an adequate transverse compliance.

Actuator pistons, as an alternative to membranes, have the disadvantage of possessing relatively large moving masses for the desired small displacements (less than 0.02 in., or 1/2 mm); this has an unfavorable effect on the transfer behavior at high frequencies. In addition, sealing problems occur, and friction forces appear on contact surfaces.

From reference 16 a relation can be derived for the force generated as a function of the fluid pressure P and the radius of the membranes R :

$$F \approx F_0 \frac{P}{P_0} \left(\frac{R}{R_0} \right)^2 \quad (2)$$

The factor F_0 is a function of the ratio of outer radius R to inner radius r and the reference magnitudes P_0 and R_0 . Setting $R/r = 3$, $P_0 = 1$ bar, and $R_0 = 1$ cm, we obtain $F_0 = 35$ N. If we then choose $R = 10$ cm and $P = 10$ bar, the force generated would be $F = 35$ kN. The membrane system has to be designed in such a manner that both the stress caused by the pressure, and the displacements are in a reasonable range. Here, a wide range of variation is given by a specific choice of parameters.

For industrial applications the frequency range (more than 200 Hz) is very important. To include the actuator system into the overall system, with the target being to design an efficient control, the input-output characteristic of the system is necessary; it is given in the x-direction as

$$T(j\omega) = \frac{F_x(t)}{u_x(t)} \quad (3)$$

where $u_x(t)$ is the control voltage (input) to the servo valve and $F_x(t)$ is the resultant force acting on the bearing housing. In the Laplace domain we can obtain the resultant force as a function of the system parameters by applying the continuity and the Bernoulli equations (under consideration of hydraulic losses), the dynamic behavior of the servo valve, and the force equilibrium at the membrane, assuming neglect of the oil compressibility. The resulting force equation is given by

$$F(s) = FV(s)U_v - F2(s)x \quad (4)$$

where

$$FV = \frac{A^* K_v}{\left(1 + \frac{2\xi_v}{\omega_v} s + \frac{s^2}{\omega_v^2} \right) K_{pq}} \quad (5)$$

$$F2 = \left(A^* C_T s^2 \right) + \left(A^* C_V \dot{x}_0 + A^* C_R + \frac{A^{*2}}{K_{pq}} \right) (s + C_M) \quad (6)$$

or by transformation into the time domain the force equation becomes

$$F^* = f_V^1 - f_2 = f_V - A^* C_T \ddot{x}_B - \left(A^* C_V \dot{x}_O + A^* C_R + \frac{A^{*2}}{K_{pq}} \right) \dot{x}_B - C_M x_B \quad (7)$$

where f_V can be obtained by the differential equation of the servo valve

$$\frac{1}{\omega_v^2} \ddot{f}_V + \frac{2\xi_v}{\omega_v} \dot{f}_V + f_V = \frac{A^* K_V}{K_{pq}} U_V \quad (8)$$

or

$$m_v \ddot{f}_V + d_v \dot{f}_V + c_v f_V = b_v U_V \quad (9)$$

The valve constants K_V , K_{pq} , the valve eigenfrequency ω_v , and the valve damping coefficient ξ_v are constants normally given by the manufacturer of the valve; A^* is the active membrane area, C_M is the membrane stiffness, C_T is a constant describing the oil inertia, C_V and C_R are constants describing fluid losses, \dot{x}_O is a characteristic flow velocity, U_V is the control voltage to the valve, and x_B is the deflection of the bearing in the force direction.

Equation (7) describes the force that is applied to the bearing, and equation (9) represents the dynamic behavior of the valve that is stimulated by the control input U_V .

An optimal design of a control system demands an adequate model of the complete system. The effectiveness of the actuator system will depend on the observability (which, in turn, depends on the measuring information) and the controllability of the natural vibrations that are to be influenced (which depends on the actuators used and their locations). In order to check on these system properties and to design an effective control system, adequate modeling is necessary.

MODELING OF ACTIVELY CONTROLLED ROTOR SYSTEMS

Modeling of Rotor Systems to be Controlled

Modeling the rotor system as a hybrid multibody system (HMBS) is a very efficient method of describing it. This has proven especially useful when active components are included. The HMBS model contains rigid bodies (e.g., bearing units) and elastic subsystems (e.g., rotors and blades), as determined by special needs (see refs. 11 and 17). The coupling of subsystems is accomplished by special elements that are characterized by the respective force laws. Modeling the system by this procedure permits the consideration of the disk mass, the shaft mass, and the gyroscopic effects in a simple manner. It also allows a modular construction of the system equations without any loss of physical insight. The procedure leads to a computer-oriented representation in which control concepts can be adequately considered. It has the advantages of low system order, versatility, and simple system adaptation (e.g., altering location of control forces acting on a flexible shaft). The equations of motion of such HMBS are best set up on a computer. A very efficient method is

the direct evaluation of the principle of d'Alembert, which can be expressed for a system consisting of k substructures as

$$\sum_{i=1}^k \int_S (\ddot{\mathbf{r}} \, dm - d\mathbf{f}^e)^T \delta \mathbf{r}_i = 0 \quad (10)$$

where the index i indicates the substructure, \mathbf{r} is the position vector to the mass element dm , $\ddot{\mathbf{r}}$ is the acceleration vector of the mass element, and $d\mathbf{f}^e$ is the force vector acting on the mass element. The symbol δ indicates the variation of the position vector \mathbf{r}_i (no variation of the time t). Rotor systems normally consist of elastic shafts and rigid bodies such as bearing housings or foundations. Taking into account the assumptions of a Bernoulli beam (cross sections of an elastic shaft remain planar), we can integrate over the mass elements in the radial direction and end up with a beam element (disk element) as shown in figure 6. (In figure 6 three different types of coordinate systems that are used in describing rotating machinery are also indicated.) As a result of this integration, equation (10) becomes

$$\sum_{i=1}^k \left\{ \int \delta \mathbf{r}_i^T (d\mathbf{m} \mathbf{a}^s - d\mathbf{f}^e)_i + \delta \boldsymbol{\varphi}_i^T (d\mathbf{I}^s \dot{\boldsymbol{\omega}} + \bar{\boldsymbol{\omega}} \, d\mathbf{I}^s \boldsymbol{\omega} - d\mathbf{M}^e)_i \right\} = 0 \quad (11)$$

Here the first term describes the virtual work of translation (in parenthesis is Newton's second law of motion), and the second term considers the virtual work of rotation (in parenthesis, Euler's equation); $\delta \mathbf{r}$ is the vector of the small virtual displacement, and $\delta \boldsymbol{\varphi}$ is the vector of the virtual rotation; \mathbf{a}^s is the vector of acceleration of the center of mass; $\boldsymbol{\omega}$ is the vector of angular velocity; $\dot{\boldsymbol{\omega}}$ is the vector of angular acceleration of the beam element; $d\mathbf{I}$ is the tensor of moment of inertia; and

$$\bar{\boldsymbol{\omega}} = \begin{bmatrix} 0 & -\omega_z & -\omega_y \\ \omega_z & 0 & -\omega_x \\ \omega_y & \omega_x & 0 \end{bmatrix} \quad (12)$$

is the skew-symmetric tensor of the angular velocities given in the system of coordinates (see fig. 6). Assuming rotational symmetry relative to the shaft axis, $d\mathbf{I}$ for the disk element can be expressed as

$$d\mathbf{I} = \begin{bmatrix} I_x & 0 & 0 \\ 0 & I_y & 0 \\ 0 & 0 & I_z \end{bmatrix} \quad (13)$$

where $I_x = I_y = \frac{I_z}{2} = \frac{dm}{16} d^2 = \frac{\rho\pi}{64} d^4(z) dz$. The torque vector acting on the beam element is represented by $d\mathbf{M}^e$. In the case of a rigid body, the integration

can be carried out over the entire body, and equation (11) would be expressed in the same manner but the differential quantities would become m , I , f^e , and M^e .

If we now introduce an $f \times 1$ vector q of the generalized minimal coordinates, where f is the number of degrees of freedom, the position vector r and the vector of the angle of twist φ can each be expressed as a function of q as follows:

$$r = r(q) \quad (14)$$

which leads to

$$\delta r = \frac{\partial r}{\partial q} \delta q$$

and

$$\varphi = \varphi(q) \quad (15)$$

which leads to

$$\delta \varphi = \frac{\partial \varphi}{\partial q} \delta q$$

Their time derivatives can be written

$$\dot{r} = \frac{\partial r}{\partial q} \dot{q} + \frac{\partial r}{\partial t} \quad (16)$$

which leads to

$$\frac{\partial \dot{r}}{\partial \dot{q}} = \frac{\partial r}{\partial q}$$

and

$$\dot{\varphi} = \omega = \frac{\partial \varphi}{\partial q} \dot{q} + \frac{\partial \varphi}{\partial t} \quad (17)$$

which leads to

$$\frac{\partial \omega}{\partial \dot{q}} = \frac{\partial \varphi}{\partial q}$$

From the relations in equations (14) to (17), equation (11) can be expressed as

$$\delta q^T \sum_i \int \left\{ \left(\frac{\partial \dot{r}}{\partial \dot{q}} \right)^T (d m a^S - d f^e) + \left(\frac{\partial \omega}{\partial \dot{q}} \right)^T (d I^S \dot{\omega} + \tilde{\omega} d I^S \omega - d M^e) \right\}_1 = 0 \quad (18)$$

where $\partial \dot{r} / \partial \dot{q} = \partial r / \partial q$ is the Jacobian matrix of translation and $\partial \omega / \partial \dot{q}$ is the Jacobian matrix of rotation. The Jacobian matrices serve as distribution matrices and can be interpreted as transformation matrices of the

forces and the torques acting on the system in such a way that the forces and torques are projected onto the directions of the generalized coordinates. We will see the usefulness of these matrices later.

A description of the system as an HMBS demands the subdivision of the generalized minimal coordinates into two types of hybrid coordinates: those with only time-dependent degrees of freedom (e.g., motion of the rigid bearing units) and those with degrees of freedom that represent elastic deformations (e.g., bending vibrations of the shafts). In the case of a shaft, the latter type describes, by distributed coordinates, the motion of the beam element shown in figure 6. These coordinates are a function of time t and the actual location of the beam element covered by the coordinate z along the rotor axis. To separate these two dependencies, we apply the Ritz product method

$$r_i(z,t) = [u(z,t), v(z,t)]^T_i = \begin{bmatrix} u^T(z) & 0 \\ 0 & v^T(z) \end{bmatrix}_i q_i(t) \quad q_i \in R^{f_i} \quad (19)$$

The vectors $u(z)$ and $v(z)$ are admissible shape functions, with f_i as the number of shape functions considered in describing the deformation of the shaft (i^{th} substructure). These vectors can be looked on as expansions of real deformations that are described by these functions. The closer these functions are to the eigenfunctions of the real system, the better is the convergence of the solution. (Note that the eigenfunctions change with the rotor frequency.) Good results have been achieved by using eigenfunctions of the nonrotating rotor, which allow a low system order even at high rotor frequencies (depending on the gyroscopic influence). The determination of these functions is carried out in a separate calculation, for example, by using cubic spline functions, Hermite polynomials, or applying finite element or experimental methods. The number of elastic degrees of freedom f_e that are chosen depends on the eigenfrequencies of the system itself and the expected excitation frequencies. The equation of motion of the separate modules (substructures) can be given in the usual form of mechanical systems

$$\begin{bmatrix} M_{xx} & 0 \\ 0 & M_{yy} \end{bmatrix}_i \ddot{q}_i + \begin{bmatrix} D_{xx} & G_{xy} \\ -G_{yx} & D_{yy} \end{bmatrix}_i \dot{q}_i + \begin{bmatrix} K_{xx} & N_{xy} \\ -N_{yx} & K_{yy} \end{bmatrix}_i q_i = h_i \quad (20)$$

The coordinates that are necessary for the description of the separate modules are included in the vector of generalized coordinates q_i . The force vector

$$h_i = \sum_j \int_0^L J_j^T f_j \delta(z - z_j) dz = \sum_j J^T(z_j) f_j \quad (21)$$

is the sum of all forces acting on the i^{th} substructure. The forces are not only imposed from outside the system, but they can also be caused by coupling effects between the subsystems. The submatrices appearing in equation (20) are displayed in table I for an axisymmetric shaft [$u(z) = v(z)$], which holds true with very few exceptions.

TABLE I. - SUBMATRICES OF ELASTIC SUBSTRUCTURES WITH RESPECT TO INERTIAL SYSTEM

Submatrices	Influence
$(\mathbf{M}_{xx})_i = (\mathbf{M}_{yy})_i = \left\{ \int_0^L \rho [A(z)u(z)u^T(z) + I_x(z)u'(z)u'^T(z)] dz \right\}_i$	Inertia
$(\mathbf{D}_{xx})_i = (\mathbf{D}_{yy})_i = d_i \left\{ \int_0^L EI_x(z)u''(z)u''^T(z) dz \right\}_i$	Material damping
$(\mathbf{G}_{xy})_i = (\mathbf{G}_{yx})_i = \left\{ 2\Omega \int_0^L \rho I_x(z)u'(z)u'^T(z) dz \right\}_i$	Gyroscopic effects
$(\mathbf{K}_{xx})_i = (\mathbf{K}_{yy})_i = \left\{ \int_0^L EI_x(z)u''(z)u''^T(z) dz \right\}_i$	Elastic forces
$(\mathbf{N}_{xy})_i = (\mathbf{N}_{yx})_i = \left\{ \int_0^L [2\Omega \rho I_x(z)u'(z)u'^T(z) + \Omega d_i EI_x(z)u'(z)u'^T(z)] dz \right\}_i$	Spin and internal damping

With equations (16) and (17), the Jacobian matrix in equation (21) can be expressed

$$\mathbf{J}_j = \frac{\partial \mathbf{r}_j(\mathbf{q}_1)}{\partial \mathbf{q}} \quad (22)$$

where

$$\mathbf{r}_j = [u(\mathbf{q}, z_j), v(\mathbf{q}, z_j)]^T$$

From equation (19), we obtain

$$\mathbf{J}(z_j) = \begin{bmatrix} \mathbf{u}^T(z_j) & 0 \\ 0 & \mathbf{v}^T(z_j) \end{bmatrix} \quad (23)$$

The vector of generalized coordinates of the overall system is

$$\mathbf{q} = [\mathbf{q}_1^T, \mathbf{q}_2^T, \dots, \mathbf{q}_k^T]^T \quad (24)$$

where $\mathbf{q} \in \mathbb{R}^f$, f is the number of degrees of freedom of the overall system, and k is the number of substructures (flexible and rigid parts). The

Jacobian matrices for the overall system relative to subsystem i can be written as

$$\bar{J}_i = \begin{bmatrix} 0_1 & 0_2 & \dots & J_i & \dots & 0_k \end{bmatrix} \quad (25)$$

The structure of these Jacobian matrices is very simple; \bar{J}_i contains only zero matrices, with one exception: J_i , which relates to the actual subsystem (ref. 11).

By formulating the system in such a way, the substructures can be combined systematically to synthesize the overall system. The Jacobian matrices serve to connect the elements. In other words, they distribute the actions of the interconnected subsystems in the matrices and thus describe the overall system. The set of equations for the whole system exhibits the structure of ordinary mechanical system equations

$$M\ddot{q} + (D + G)\dot{q} + (K + N)q = h \quad q \in R^f \quad (26)$$

By introducing the state space vector

$$x(t) = \begin{bmatrix} q^T, \dot{q}^T \end{bmatrix}^T \quad (26a)$$

where $x \in R^n$ and $n = 2f$, equation (26) becomes

$$\dot{x} = Ax + Bu \quad (26b)$$

where $A \in R^{n,n}$ and $B \in R^{n,r}$; f is the number of degrees of freedom; r , the number of actuators; and u , the control vector.

Using this method to model systems consisting of rigid and elastic subsystems has proven to be very suitable, especially when considering active elements. The advantage of this method, compared to others, is the low system order resulting from always using a Ritz approximation, which takes the mode shapes of the nonrotating rotor as admissible shape functions. Using these functions for the Ritz series provided very fast convergence, even at high rotor frequencies. For this reason the calculation expense is always low, even for very complicated rotor structures.

Modeling of the Complete System

To design a control system, it is necessary to include the actuators in the system model. The differential equation must be represented in such a form that the right side of the equation contains only terms that are influenced by the controller (disturbance forces can always be added easily).

The differential equation, especially the resulting changes in the system matrices, must be tailored to the electromagnetic actuators acting both directly on the rotor and via the bearing housings, and also to the active chamber system.

Inclusion of electromagnetic actuators. - We start with the following differential equation:

$$M\ddot{q}(t) + P\dot{q}(t) + Qq(t) = \Sigma_j h_j(q, \dot{q}, \ddot{q}, \Omega, T, t) \quad (26)$$

where Ω is the rotor frequency, T is the oil temperature when using journal bearings, and t indicates the time. By using electromagnetic actuators to apply forces directly on the rotor,

$$h_j = \int_0^L J_R^T f_j \cdot \delta(z - z_j) dz = J_R^T(z_j) f_j \quad (27)$$

where J_R is the Jacobian matrix of translation for the subsystem flexible rotor; f_j is the discrete force vector (here control force) acting on the rotor at the location z_j ; and $\delta(z - z_j)$ is the Dirac function that permits the consideration of the discrete location of z_j (screening characteristic of the Dirac function).

Alternatively, we can apply forces that act indirectly (via the rigid bearing housings) on the rotor

$$h_B = J_B^T f_B \quad (28)$$

where J_B is the Jacobian matrix of the subsystem rigid bearing element and f_B is the force vector acting on this bearing element. Combining equations (1) and (28), we can formulate

$$J_B^T \begin{bmatrix} F_x \\ F_y \end{bmatrix} = J_B^T \begin{bmatrix} k & 0 \\ 0 & k \end{bmatrix} \begin{bmatrix} x \\ y \end{bmatrix} + J_B^T \begin{bmatrix} k_i & 0 \\ 0 & k_i \end{bmatrix} \begin{bmatrix} i_x \\ i_y \end{bmatrix} = k J_B^T J_B q + k_i J_B^T i \quad (29)$$

In this formulation we took advantage of equations (14) and (16) to express the x-, y-movement of the bearing by using the vector q of the generalized coordinates and the Jacobian matrix of translation belonging to the subsystem bearing element, which is expressed as

$$r_B = [x, y]^T = J_B q \quad (30)$$

When a magnetic bearing acting directly on the rotor is applied at location z_j , equation (30) becomes

$$r_j = [u(z_j, t), v(z_j, t)]^T = J_R(z_j) q \quad (31)$$

The equation of the complete system can be achieved by integrating the force equation (29) into the differential equation (26a)

$$M\ddot{q} + P(\Omega)\dot{q} + [Q(\Omega) - k J_B^T J] q = B u \quad (32)$$

where $B = k_1 k_0 J_B$ is the control matrix with k_0 as the gain coefficient of the power amplifier, and u is the control vector containing the input voltages to the power amplifier. The negative sign of the term $k J_B^T J_B$ indicates the negative stiffness produced by the magnetic actuator.

Inclusion of active chamber system. - The active chamber system (hydraulic actuator) is described by the force equation (8). We introduce the abbreviation

$$f = f_V - \bar{m}\ddot{x}_B - \bar{d}\dot{x}_B - c_B x_B \quad (33)$$

and use the equation of the servo valve described by

$$m_V \ddot{f}_V + d_V \dot{f}_V + c_V f_V = b_V U_V \quad (9)$$

as already given. The system order increases by one degree of freedom for each servo valve, so the vector of generalized coordinates, q , has to be enlarged by the two additional coordinates, f_{Vx} and f_{Vy} (for the servo valves serving the x - and y -directions respectively):

$$\bar{q} = [q^T, f_{Vx}, f_{Vy}] \quad (34)$$

The resulting differential equation, in conjunction with equations (31), (33), and (9), can be expressed as

$$\begin{bmatrix} M & 0 & 0 \\ 0 & m_V & 0 \\ 0 & 0 & m_V \end{bmatrix} \ddot{\bar{q}} + \begin{bmatrix} P & 0 & 0 \\ 0 & d_V & 0 \\ 0 & 0 & d_V \end{bmatrix} \dot{\bar{q}} + \begin{bmatrix} Q & 0 & 0 \\ 0 & c_V & 0 \\ 0 & 0 & c_V \end{bmatrix} \bar{q} = \bar{J}_B^T \begin{bmatrix} f_{Vx} & -\bar{m}\ddot{x}_B & -\bar{d}\dot{x}_B & -c_B x_B \\ f_{Vy} & -\bar{m}\ddot{y}_B & -\bar{d}\dot{y}_B & -c_B y_B \end{bmatrix} + b_V \bar{J}_V^T \begin{bmatrix} U_{Vx} \\ U_{Vy} \end{bmatrix} \quad (35)$$

The coefficients \bar{m} , \bar{d} , and c_B describe the additional mass, damping, and stiffness effects caused by the actuator system; \bar{J}_B is the enlarged Jacobian matrix of translation for the subsystem bearing, and \bar{J}_V is the Jacobian matrix belonging to the subsystem servo valve. Those terms of equation (36) that are multiplied by J_B are linearly dependent on the system coordinates and thus contribute to the homogeneous terms of the differential equations (dynamic behavior of the complete system).

The radial movement of the bearing, described by x_B and y_B , and the servo valve dynamics, described by coordinates f_{Vx} and f_{Vy} , can be expressed by the enlarged Jacobian matrices of the subsystem (ref. 11)

$$\begin{bmatrix} x_B \\ y_B \end{bmatrix} = \bar{J}_B \bar{q} \quad (36)$$

and

$$\begin{bmatrix} f_{Vx} \\ f_{Vy} \end{bmatrix} = \bar{J}_V \bar{q} \quad (37)$$

The final formulation of the differential equation of the complete system can be given as

$$\left[\bar{M} + \bar{J}_B^T \bar{J}_B \bar{m} \right] \ddot{\bar{q}} + \left[\bar{P} + \bar{J}_B^T \bar{J}_B \bar{d} \right] \dot{\bar{q}} + \left[\bar{Q} + \bar{J}_B^T \bar{J}_B c_B - \bar{J}_B^T \bar{J}_V \right] \bar{q} = Bu \quad (38a)$$

or

$$\hat{M} \ddot{\bar{q}} + \hat{P} \dot{\bar{q}} + \hat{Q} \bar{q} = Bu \quad (38b)$$

One can see that the coupling of the mechanical system, the fluid system, and the electrical system can be managed very elegantly. The Jacobian matrices that are involved serve as the "distribution-matrices." They distribute the interaction of the involved subsystem.

The input by the actuator is characterized by the term Bu where B is the control matrix, which depends to a high degree on the actuator locations chosen, and u is the $r \times 1$ control vector with r as the number of actuators involved.

If we use a linear combination of all imaginable measurements (displacements q , velocities \dot{q} , accelerations \ddot{q} , and integrated displacements q_I), the control vector can be expressed as

$$u = -KC \left[\bar{q}_I^T, \bar{q}^T, \dot{\bar{q}}^T, \ddot{\bar{q}}^T \right]^T = -K\bar{x} \quad (39a)$$

or

$$u = - \left[K_I \mid K_P \mid K_D \mid K_A \right] C\bar{x} \quad (39b)$$

where K_I is the gain matrix relative to $q_I = \int q dt$; K_P is the gain matrix with respect to the displacement vector; K_D is the gain with relation to the velocities; K_A is the feedback matrix taking into account the accelerations; and C is the measurement matrix, which takes into account that often not all displacements with their time derivatives and integrals are known. The relation between an enlarged vector

$$\bar{x} = \left[\bar{q}_I^T, \bar{q}^T, \dot{\bar{q}}^T, \ddot{\bar{q}}^T \right]^T \quad (40)$$

and the measurement vector y can be given as

$$y = C\bar{x} \quad (41)$$

With equation (39a), equation (38b) can be formulated as

$$(\hat{M} + BK_A C)\ddot{\bar{q}} + (\hat{P} + BK_D C)\dot{\bar{q}} + (\hat{Q} + BK_P C)\bar{q} + BK_I Cq_I = 0 \quad (42)$$

For several reasons it is more convenient to transform equation (42) into the state space representation. By introducing a state space vector

$$x = [\bar{q}_I^T, \bar{q}^T, \dot{\bar{q}}^T]^T \quad (43)$$

(where x is different from the normally used state space vector because it has been enlarged by the vector q_I , which contains the integrated displacement coordinates) equation (42) becomes

$$\begin{bmatrix} \dot{\bar{q}}_I \\ \dot{\bar{q}} \\ \ddot{\bar{q}} \end{bmatrix} = \begin{bmatrix} 0 & E & 0 \\ 0 & 0 & E \\ -M_A^{-1}BK_I C & -M_A^{-1}(\hat{P} + BK_D C) & -M_A^{-1}(\hat{Q} + BK_P C) \end{bmatrix} \begin{bmatrix} \bar{q}_I \\ \bar{q} \\ \dot{\bar{q}} \end{bmatrix} \quad (44)$$

or

$$\dot{x} = \hat{A}x \quad (45)$$

Equation (42) shows that the mass matrix M_A is a function of the acceleration feedback characterized by K_A :

$$M_A = \hat{M} + BK_A C \quad (46)$$

In the case of acceleration feedback - this depends on the software available - using the second order equation (42) for optimization of the controller can be advantageous because of the controller-dependent mass matrix

$$M_A = M_A(K_A) \quad (47)$$

Discussion of Several Cases

Proportional derivative (PD) controller. - In this case, where $K_p \neq 0$, $K_D \neq 0$, $K_A = 0$, and $K_I = 0$, M_A is constant; however, because $K_I = 0$ (no integral term), the system can be reduced to the usual form (the $f_I \times 1$ vector q_I in the state space vector x can be canceled). This means the upper f_I rows and the f_I columns at the left side of the system matrix A can be canceled.

Proportional derivative-acceleration (PDA) controller. - Here, $K_p \neq 0$, $K_D \neq 0$, $K_A \neq 0$, and $K_I = 0$. The reduced order system (PD controller) is still valid here, but the mass matrix is a function of the acceleration feedback [$M_A = M(K_A)$].

Proportional integral derivative-acceleration (PIDA) controller. - In this case, all submatrices appearing in K (see eq. (39)) are nonzero. And for calculation (optimization and simulation), the enlarged system described by the differential equation (45) - full order system - has to be taken into account.

From the complete description of the system, the design of suitable control concepts can be achieved. The effectiveness of the controller, in connection with the actuators and sensors used, depends to a high degree on the controllability and observability conditions of the system. These system properties will be discussed in the following section.

CONTROLLABILITY, OBSERVABILITY AND SPILLOVER

Controllability and Observability

Controllability and observability are two of the most important factors in the theory of dynamic systems. They play a very important role when designing a control system and give an insight into the physical problem. Simply put, controllability means the ability to adequately control the dynamic behavior of the system through the actuators used. Observability means that appropriate sensors exist at appropriate locations such that the pertinent dynamic behavior can be detected. The controllability and the observability of the system are mainly determined by the chosen actuators and sensors and their locations. Controllability and observability can change as a function of rotor speed, stiffness and damping of the bearings, oil temperature of the fluid film (in the case of journal bearings), and so on. Much software is available to check on these system properties. For time-invariant mechanical systems, the Hautus and the Kalman criteria are generally used (see refs. 17 and 18).

The controllability and/or observability can be studied via the mode shapes (eigenvectors) of the system. This can be explained on a simple system whose mechanical model is shown in figure 7. When one uses control forces, the controllability is indicated by the amplitudes of the various mode shapes at the actuator location. This means the larger the amplitude, the higher the controllability. For illustration, the mode shapes up to the fourth order are displayed in figure 8 for the system shown in figure 7 for two different rotor frequencies ($\Omega = 0$ and $\Omega = 100$ Hz). Only one set of modes appears when $\Omega = 0$ (fig. 8(b): symmetrical system, decoupling in x- and y-direction). The modes split at rotor frequencies $\Omega \neq 0$ into forward and backward modes (figs. 8(c) and (a) respectively).

By applying forces that act directly on the rotor (with a magnetic bearing), all natural mode shapes of the rotor could be influenced sufficiently if the forces acted at locations where the amplitudes of the modes have their maximum value. Unfortunately, this maximum occurs at different places for different modes, and the modes can also be influenced by the rotor frequency (compare the forward and backward modes at $\Omega = 100$ Hz, gyro influence). The optimal actuator location depends on one's objectives, and it will always be a compromise.

Now consider the rotor to be supported by roller or journal bearings. The vibration behavior is to be improved by control forces via bearing housings

(indirectly acting on the rotor). In this case the effectiveness, that is, the controllability, is characterized to a large extent by the stiffness of the bearings and also by the bearing support stiffness.

For some idea of these influences see figure 9; it shows a measure of the controllability for the first and the third forward modes of the system in figure 7. As a measure of controllability, one can use the square or any other suitable norm of the bearing displacement at the actuator location. In each case the controllability is plotted as a function of the bearing stiffness c_k and the bearing support stiffness c_a relative to the stiffness c_w of the rotor itself. In figure 9(a) the controllability can be seen to decrease with reduced c_k . Physically, this result is very understandable; the lower the stiffness between bearing and shaft, the smaller the effectiveness of control forces acting via the bearings. The behavior with respect to the outer bearing support stiffness is the opposite. Although not shown, these results are similar for the second forward mode but are not valid in general. The controllability of the third forward natural mode (bearing displacement) is plotted in figure 9(b). This behavior is different from the preceding one because of increasing influence of inertia with rising frequency of oscillation.

For the example under consideration, good controllability of the important natural mode shapes (up to the third order) in the current frequency range is guaranteed if the stiffnesses satisfy the conditions

$$\frac{c_k}{c_w} > 1 \quad \text{and} \quad \frac{c_a}{c_w} < 1 \quad (48)$$

Investigations of the observability are similar, and for the system under consideration the results are identical.

Spillover

If elastic components are involved in the system, an exact system description requires an infinite number of shape functions. In practice, only a finite number of modes can be considered, and in fact, only a few are needed for adequate control. The consequences of this incomplete system description are spillover effects.

Spillover effects can appear on two different levels. On the one level, the measurements contain both the modes considered in the model and also the modes that have been disregarded. Both sets of modes influence the signals at the measurement locations; this leads to observation spillover. On the other level, control forces may destabilize modes of higher order that have not been accounted for in the control design, thereby leading to control spillover. Usually, internal damping is assumed to be large enough to prevent instabilities due to spillover effects. Because this is not true in every case, it is prudent to consider these effects in the control design. Theoretical investigations lead to the collocation condition (refs. 5 and 20)

$$B = C^T \quad (49)$$

where B is the control matrix (eq. (26 b)) and C is the measurement matrix

(eq. (41)). The condition given by equation (49) requires that actuators and sensors be located at the same place. It also requires only velocity feedback; the number of signals involved in the feedback must be equal to the number of actuators used.

For economic reasons, using more signals than actuators in order to receive as much information as possible about the system seems quite reasonable. In fact, an improvement of the dynamic behavior is often possible if we use more sensors than actuators. To avoid instabilities, the neglected mode shapes in the system description must be neither observable nor controllable. These requirements lead to a practical criterion for the choice of the actuator and sensor locations, which is expressed by the following equations:

$$\sum_i |v_i(z_S)| \rightarrow \min \quad i > n_n \quad (50)$$

and

$$\sum_i |v_i(z_A)| \rightarrow \min \quad i > n_n \quad (51)$$

where z_S is the position of the sensors, z_A , the actuator location, and n_n , the number of shape functions considered in the system description. Reference 5 provides hints on managing the simulation of such a system.

Minimal spillover can be expected if at the actuator locations the amplitudes of the higher modes tend to zero. Often, suitable positions may be found directly by evaluating the eigenfunctions (fig. 10). For systems with large mass concentrations, the high-order natural vibrations have almost no corresponding rigid body motions. Only the low-order relevant vibrations contain significant rigid body movements in addition to elastic deformations. Therefore, we recommend placing the actuators and sensors at the points of mass concentration where, in practice, the higher order eigenfunctions have none or only small displacements. When we take a closer look at the mode shape with a frequency of 2100 Hz (fig. 10), we can see that to avoid spillover, the sensor should pick up the bearing movement and not the movement of the rotor at the bearing location.

Spillover effects may also be due to sensor locations and actuator locations not being the same. For example, two rotor modes are illustrated in figure 10. For the first mode, the rotor moves in the same direction at both the sensor location and the actuator location. For the second mode, the rotor moves in opposite directions at the two locations. This means that, for first mode motion, a positive x-displacement at the sensor requires a negative x-force at the actuator to counteract it. However, for the second mode, a positive x-displacement requires a positive x-force to counteract it. That is, the relation between sensor motion and required actuator force is opposite for the two modes. If the controller gain is assumed constant at all frequencies, and the controller is programmed to suppress first-mode vibration, then the second mode will be unstable. This occurs because the actuator response is to increase the second mode motion rather than to suppress it.

Spillover can also be shown analytically as follows. Consider the case when velocities \dot{x}_S and \dot{y}_S are taken at location z_S with the gains $k_x = k_y = k$ and without coupling between the x- and y-directions. Then for control forces generated by a magnetic bearing located at plane M, we obtain

$$\mathbf{f}_M = \begin{bmatrix} f_{Mx} \\ f_{My} \end{bmatrix} = - \begin{bmatrix} k_x & 0 \\ 0 & k_y \end{bmatrix} \begin{bmatrix} \dot{x} \\ \dot{y} \end{bmatrix} = -kJ(z_S) \begin{bmatrix} \dot{q}_x \\ \dot{q}_y \end{bmatrix} \quad (52)$$

For a demonstration of spillover effects, only two modes will be considered (that is, two in each direction); see equation (19). The number of degrees of freedom f is 4. The vectors of the admissible shape functions become (compare with fig. 11)

$$\mathbf{u}(z) = \mathbf{v}(z) = \begin{bmatrix} u_1 \\ u_2 \end{bmatrix} = \begin{bmatrix} \sin \frac{\pi z}{L} \\ \sin \frac{2\pi z}{L} \end{bmatrix} \quad (53)$$

The sine functions in the sample considered are the eigenfunctions of the non-rotating rotor. For inclusion of the force vector \mathbf{f}_M (eq. (21)) in the differential equations given by equation (20), the force vector can be expressed

$$\mathbf{h} = -kJ^T(z_M)J(z_S) \begin{bmatrix} \dot{q}_x \\ \dot{q}_y \end{bmatrix} \quad (54)$$

With equation (53), the Jacobian matrices appearing in equation (54) can be given explicitly as

$$\mathbf{J}_M = \begin{bmatrix} u_{M1} & u_{M2} & 0 & 0 \\ 0 & 0 & u_{M1} & u_{M2} \end{bmatrix} \quad \text{and} \quad \mathbf{J}_S = \begin{bmatrix} u_{S1} & u_{S2} & 0 & 0 \\ 0 & 0 & u_{S1} & u_{S2} \end{bmatrix} \quad (55)$$

If we take $z_M = L/4$ and $z_S = (3/4)L$, we obtain $u_{M1} = u_{S1} = \sqrt{2}/2 = a > 0$ and $u_{M2} = -u_{S2} = 1 = b > 0$. The spillover effects can be explained analytically if we set the rotor frequency $\Omega = 0$. In this case, equation (20) is decoupled in the x - and y -directions (see table I). Assuming the runner consists of a thin disk with mass m and radius r , the thickness b of the disk is much less than the length L of the shaft, and the shaft is massless, then equation (20) can be written in the x -direction as

$$m \begin{bmatrix} 1 & 0 \\ 0 & \frac{2\pi^2 r^2}{L^2} \end{bmatrix} \begin{bmatrix} \ddot{q}_1 \\ \ddot{q}_2 \end{bmatrix} + k \begin{bmatrix} a^2 & -ab \\ ab & -b^2 \end{bmatrix} \begin{bmatrix} \dot{q}_1 \\ \dot{q}_2 \end{bmatrix} + \begin{bmatrix} c_1 & 0 \\ 0 & c_2 \end{bmatrix} \begin{bmatrix} q_1 \\ q_2 \end{bmatrix} = 0 \quad (56)$$

Note that equation (56) represents only half of the system. The other half (in the y -direction) is the same because of rotational symmetry.

The stability of the system can be verified by the characteristic equation relative to equation (56)

$$Am\lambda^4 + (ka^2A - mkb^2)\lambda^3 + (c_2m + c_1A)\lambda^2 + (c_2ka^2 - c_1kb^2)\lambda + c_1c_2 = 0 \quad (57)$$

where $A = 2\pi^2 r^2 m / L^2$. By the Stodola criterion (ref. 18), the system is unstable if the coefficient of λ and/or λ^3 is less than zero. The coefficient of λ is

$$a_1 = k(a^2 c_2 - b^2 c_1) \quad (58a)$$

and the coefficient of λ^3 is

$$a_3 = k(a^2 A - mb^2) \quad (58b)$$

From table I and equation 53, we obtain

$$c_1 = \left(\frac{\pi}{L}\right)^4 EI \int_0^L \sin^2 \frac{\pi z}{L} dz = \left(\frac{\pi}{L}\right)^4 EI \left(\frac{L}{2}\right) \quad (59a)$$

and

$$c_2 = 16 \left(\frac{\pi}{L}\right)^4 EI \int_0^L \sin^2 \frac{2\pi z}{L} dz = 16 \left(\frac{\pi}{L}\right)^4 EI \left(\frac{L}{2}\right) \quad (59b)$$

Combining equations (59a) and (59b), we obtain

$$c_2 = 16c_1 > 0 \quad (60)$$

Since $b^2 = 2a^2 > 0$, it follows that if $k > 0$

$$a_1 > 0 \quad (61)$$

As a result of equation (61), we know, for positive k , that the system can only be unstable if $a_3 < 0$. If $L/r > \pi$, this condition is fulfilled and the system becomes unstable. (If $k < 0$, then $a_1 < 0$ and the system is unstable for any value of L/r .)

CONTROL CONCEPTS AND CONTROLLER OPTIMIZATION

The design of linear and nonlinear controllers, both analog and digital, has been treated in great detail in the literature. There are numerous methods and concepts for the design and realization of controllers. The choice of a concept is determined mainly by the aim and the physical realities of the plant (i.e., the open loop). In the following, only a time invariant and linear system is assumed:

$$\dot{x}(t) = A(\Omega, \dot{\Omega}, t, T)x(t) + Bu(t) \quad A \in R^{n,n} \quad \text{and} \quad B \in R^{n,r}$$

and

$$y(t) = Cx(t) \quad C \in R^{m,n} \quad (62)$$

Here, A is the system matrix; B , the control matrix (dependent on the actuator locations and actuator type); C , the measurement matrix (dependent on the

measurement locations and the type of sensors used); $n = 2f$, the system order, where f is the number of degrees of freedom; r , the number of independent forces generated by the actuators; m , the number of signals used to realize the feedback (measurement coordinates); Ω , the rotor frequency; $\dot{\Omega}$, its time derivative; and T , the oil temperature.

Depending on the information used, two concepts may be distinguished: state feedback

$$u(t) = K_S(\Omega, T)x(t) \quad K_S \in R^{r, n} \quad (63)$$

and output feedback

$$u(t) = K_O(\Omega, T)y_M(t) \quad K_O \in R^{r, m} \quad (64)$$

This means that the control vector u is a linear function of either the system state vector $x(t)$ or of the system output, that is, the measurement vector $y_M(t)$, which is directly available from the system sensors.

State Feedback Control

In designing a state feedback controller, the following methods are generally used:

- (1) Optimization according to the quadratic integral criterion (or performance index):

$$J = \int_0^{\infty} (x^T Q x + u^T R u) dt \rightarrow \min \quad (65)$$

This criterion takes into account all coordinates for describing the system represented by x and for the system output given by u as well. By using this approach, the design problem is reduced to the task of solving the algebraic Riccati equation (ref. 11). The weak point in this procedure is the adaption of the weighting matrices Q and R for the specific problem.

- (2) Choice of the eigenvalues λ_i of the closed control loop (pole assignment):

$$[\lambda_i E - (A - BK)] \bar{q} = 0 \quad (66)$$

In contrast to the previous method, the choice of suitable eigenvalues (poles) is the problem with this approach. With the selection of eigenvalues, a specific system behavior is enforced, so in the case of poorly adapted values, extremely high control forces may appear. The influence of gyroscopic effects may even worsen the system dynamics. Hints on choosing suitable poles are given in reference 21.

- (3) Modal state control

This method allows for a shift of one or more eigenvalues. This can be especially useful for rotor systems that, for whatever reasons, are run in the

vicinity of resonances. With the control concept given in the following, however, one can only shift as many poles as there are actuators (refs. 5 and 21). In the control design state, the system (eq. (62)) is transformed into

$$\dot{\bar{x}}(t) = \Lambda \bar{x}(t) + T^{-1}Bu(t) = [\Lambda - K_M]\bar{x}(t) \quad (67)$$

The matrix Λ is real and has a diagonal block structure (ref. 11). The gain matrix K_S appearing in equation (63), which is needed to realize results, is given by

$$K_S = B^+TK_M T^{-1} \quad (68)$$

with

$$B^+ = (B^TB)^{-1}B^T \quad (69)$$

being the pseudoinverse of the column regular control matrix B from equation (62).

(4) Combined state feedback control

This kind of control is useful in cases where the application of a controller that was designed according to method (1) or (2) does not yield sufficient damping of some natural vibrations. Here the additional application of a modal feedback control according to method (3) can improve the system behavior significantly. The additional effort for this case is negligible since a summation of gain matrices affects only the gain coefficients, whereas the structure of the controller remains the same.

Output Feedback Control

With a limited number of measurements, the possible influence on system behavior is restricted. However, the obtainable results are still sufficient for most applications. Significant improvement by means of state feedback often requires a large number of sensors, which in most cases is not practical.

The design of an output feedback control always implies a parameter optimization, that is, an optimal tuning of the coefficients of the feedback matrix in equation (64). If we design an output feedback with the quadratic quality criterion, the quality functional can be acquired by solving the Ljapunov matrix equation. Utilizing all symmetry characteristics reduces the number of variable parameters significantly, thereby decreasing the calculation expense as well.

It is important to note that in contrast to the Riccati controller, different initial conditions $x(t_0) = x_0$ will result in different optimal control matrices K_0 . The initial conditions may be set explicitly in such a way as to enforce consideration of some critical natural mode shapes (e.g., by equating x_0 to a specific eigenvector characterizing a natural mode shape).

Under certain circumstances (i.e., when fully observable and controllable) the output feedback control allows for shifting of specific eigenvalues as well. If the modal description of the system is as in equation (67), the feedback matrix K_0 in equation (64) becomes

$$K_0 = B^+TK_M T^{-1}C^+ \quad (70)$$

with

$$C^+ = C^T(CC^T)^{-1} \quad (71)$$

being the pseudoinverse of the row regular measurement matrix C in equation (62). In general, the matrix C is not square so it cannot be inverted; thus the pseudoinverse indicated in equation (71) must be used. This means that the other poles are shifted as well, and a check on the stability and system behavior after the shift of the poles is required (refs. 21 and 22).

EXAMPLES AND RESULTS

Knowing how to construct a controller and which type of controller to chose depends to a high degree on one's objectives. In this section, several examples will be given to demonstrate the design procedures.

Magnetic Suspension of an Epitaxy Centrifuge

The information in this section is taken from reference 1. The rotor system was developed for application in liquid-phase epitaxial growth of very thin semiconductor layers. In order to obtain layers of high quality, a very smooth rotation is required in a reactor that is leakproof even under ultra-high-vacuum conditions. An active suspension of the rotor was necessary in order to absolutely exclude contamination by lubricants or by wear.

The resulting epitaxy centrifuge, supported without contact, is shown in figure 12. The upper part of the apparatus contains the rotating crucible where the epitaxial layers grow. The crucible can be heated up to 1000 K by a furnace. The supporting unit is concentrated in the lower framework. The rotor spins without contact in the vacuum tube. The bearings, the attitude sensors, and the stator of the electric drive have to be outside the tube to prevent contamination. Bearing forces, attitude signals, and driving torque are transmitted through the walls of the tube. Two emergency bearings prevent damage of the rotor in case of a magnetic bearing failure.

Equations of motion and state. - The mechanical model that is the basis of the system described is shown in figure 13. The elongated rotor is assumed to be rigid. Asymmetries of the rotor are restricted to small dynamic and static unbalances only. The driving torque acts about the rotor axis. The radial bearings exert discrete horizontal control forces; the axial bearing force acts along the rotor axis. The axial bearing's vertical force component compensates for the rotor weight $m \cdot g$; its horizontal components act like an elastic restoring force. The deviation of the rotor from its vertical reference position is described by the given vector $r(t)$ and the small inclination angles α and β , as indicated in figure 13. Linearization of the equations of motion is justifiable. As a consequence, the horizontal motion is decoupled from the vertical motion.

Because the rotor is assumed to be rigid, the four degrees of freedom of the radial motions can be described by the four coordinates x and y

(translational) and α and β (rotational). The vector of generalized coordinates for describing the dynamic behavior of the rotor can be taken as

$$\mathbf{q} = [x, \beta, y, -\alpha]^T \quad (72)$$

where x and y are radial displacements of the rotor at point S shown in figure 13. The negative sign of the angle α can be explained by the displacements in the y -direction that are caused as a result of angular movement α . These displacements at the locations $z_1 = L_U$ or $z_2 = L_O$ are positive if α is negative.

From equation (19) we obtain the vector of the admissible shape function,

$$\mathbf{u}(z) = \mathbf{v}(z) = [1, z]^T \quad (73)$$

or the displacement vector as a function of the coordinate z along the rotor axis,

$$\mathbf{r}(z, t) = \begin{bmatrix} 1 & 0 \\ 0 & z \end{bmatrix} \begin{bmatrix} x \\ \beta \\ y \\ -\alpha \end{bmatrix}^T \quad (74)$$

or in connection with equation (14),

$$\mathbf{r}(z, t) = \frac{\partial \mathbf{r}}{\partial \mathbf{q}} \mathbf{q} = \mathbf{J}_T \mathbf{q} \quad (75)$$

with \mathbf{J}_T as the Jacobian matrix of translation. The Jacobian matrix of rotation appearing in equation (18) can be expressed

$$\frac{\partial \boldsymbol{\omega}}{\partial \dot{\mathbf{q}}} = \frac{\partial [\dot{\alpha}, \dot{\beta}]^T}{\partial \dot{\mathbf{q}}} = \begin{bmatrix} \frac{\partial \dot{\alpha}}{\partial \dot{x}} & \frac{\partial \dot{\alpha}}{\partial \dot{\beta}} & \frac{\partial \dot{\alpha}}{\partial \dot{y}} & \frac{\partial \dot{\alpha}}{\partial (-\dot{\alpha})} \\ \frac{\partial \dot{\beta}}{\partial \dot{x}} & \frac{\partial \dot{\beta}}{\partial \dot{\beta}} & \frac{\partial \dot{\beta}}{\partial \dot{y}} & \frac{\partial \dot{\beta}}{\partial (-\dot{\alpha})} \end{bmatrix} = \mathbf{J}_R \quad (76)$$

Radial forces acting on the rotor. - These are forces generated by the active elements and the weight of the rotor at the locations $z = L_U, S, L_O, L_A$ (fig. 13). The force vector of equation (21) can be given as

$$\mathbf{h} = \mathbf{J}_T^T(L_U) \mathbf{f}_{Mu} + \mathbf{J}_T^T(L_O) \mathbf{f}_{Mo} + \mathbf{J}_T^T(L_A) \mathbf{f}_A + \mathbf{J}_R^T \mathbf{t}_c \quad (77)$$

and \mathbf{f}_{Mu} and \mathbf{f}_{Mo} are given by the magnetic bearing equation

$$\mathbf{f}_{Mu, o} = \begin{bmatrix} f_x \\ f_y \end{bmatrix}_{u, o} = \begin{bmatrix} k_{sx} & 0 \\ 0 & k_{sy} \end{bmatrix} \begin{bmatrix} x \\ y \end{bmatrix}_{u, o} + \begin{bmatrix} k_i & 0 \\ 0 & k_i \end{bmatrix} \begin{bmatrix} i_x \\ i_y \end{bmatrix}_{u, o} \quad (78)$$

or

$$\mathbf{f}_j = k_s \mathbf{J}_T(z_j) \mathbf{q} + k_i \mathbf{i}_j$$

The radial component of the axial magnetic bearing can be considered as a restoring force

$$\mathbf{f}_A = \begin{bmatrix} f_{Ax} \\ f_{Ay} \end{bmatrix} = -k_m \begin{bmatrix} x_A \\ y_A \end{bmatrix} = -k_m \mathbf{J}_T^T(a_A) \mathbf{q} \quad (79)$$

with k_m as a bearing constant.

Eventually, the torque t_c produced by the couple of forces consisting of weight G and the axial force F_{AZ} for compensating the weight can be given as

$$\mathbf{t}_c = -mg \begin{bmatrix} \alpha(L_A - s) \\ \beta(L_A - s) \end{bmatrix} = -mg(L_A - s) \mathbf{J}_R \mathbf{q} \quad (80)$$

Combining equation (78) with equation (80), we obtain

$$\mathbf{h} = \left[\left(\mathbf{J}_T^T(L_U) \mathbf{J}_T(L_U) + \mathbf{J}_T^T(L_O) \mathbf{J}_T(L_O) \right) k_s - k_m \mathbf{J}_T^T(L_A) \mathbf{J}_T(L_A) - mg(L_A - s) \mathbf{J}_R^T \mathbf{J}_R \right] \mathbf{q} + \mathbf{B} \mathbf{u} \quad (81)$$

where

$$\mathbf{u} = [i_{x0}, i_{xu}, i_{y0}, i_{yu}]^T \quad (82)$$

is the control vector built up by the control currents in the given order. With regard to equation (78), the control matrix \mathbf{B} has to be

$$\mathbf{B} = \begin{bmatrix} \bar{\mathbf{B}} & \mathbf{0} \\ \mathbf{0} & \bar{\mathbf{B}} \end{bmatrix} \quad \bar{\mathbf{B}} = k_1 \begin{bmatrix} 1 & 1 \\ a_0 & a_u \end{bmatrix} \quad (83)$$

The matrices of the system

$$\mathbf{M} \ddot{\mathbf{q}} + \mathbf{P} \dot{\mathbf{q}} + \mathbf{K} \mathbf{q} = \bar{\mathbf{B}} \mathbf{u} \quad (84)$$

can be calculated from table I and the vector of the admissible shape functions (eq. (73)) as follows:

$$\mathbf{M} = \begin{bmatrix} m & ms & 0 & 0 \\ ms & A + ms^2 & 0 & 0 \\ 0 & 0 & m & ms \\ 0 & 0 & ms & A + ms^2 \end{bmatrix} \quad \mathbf{P} = \begin{bmatrix} 0 & 0 & 0 & 0 \\ 0 & 0 & 0 & I_z \\ 0 & 0 & 0 & 0 \\ 0 & -I_z & 0 & 0 \end{bmatrix}$$

$$K = \begin{bmatrix} -2k_{sx} + k_m & L_A k_m - (L_O + L_U) k_{sx} & 0 & 0 \\ -(L_O + L_U) k_{sx} & mg(L_A - s) + L_A^2 k_m & 0 & 0 \\ + L_A k_m & - (L_U^2 + L_O^2) k_{sx} & -2k_{sy} + k_m & L_A k_m - (L_O + L_U) k_{sy} \\ 0 & 0 & -(L_O + L_U) k_{sy} & mg(L_A - s) + L_A^2 k_m \\ 0 & 0 & + L_A k_m & - (L_U^2 + L_O^2) k_{sy} \end{bmatrix}$$

$$\bar{B}u = \begin{bmatrix} k_{1x} & k_{1x} & 0 & 0 \\ L_O k_{1x} & L_U k_{1x} & 0 & 0 \\ 0 & 0 & k_{1y} & k_{1y} \\ 0 & 0 & L_O k_{1y} & L_U k_{1y} \end{bmatrix} \begin{bmatrix} i_{x0} \\ i_{xu} \\ i_{y0} \\ i_{yu} \end{bmatrix} \quad (85)$$

Introducing the state vector $x = [q^T, \dot{q}^T]^T$, we obtain the state equation

$$\dot{x} = Ax + Bu \quad A = \begin{bmatrix} 0 & E \\ -M^{-1}K & -M^{-1}P \end{bmatrix} \quad \text{and} \quad B = \begin{bmatrix} 0 \\ M^{-1}\bar{B} \end{bmatrix} \quad (86)$$

The essential values of the design parameters of the centrifuge are given in table II.

TABLE II. - DESIGN PARAMETERS OF CENTRIFUGE

Coordinates, m	
L_O	0.314
L_U	0.126
s	0.458
L_A	0.448
Moments of inertia, kgm^2	
Transverse, I_y	0.060
Polar, I_z	0.00421
Mass, m, kg	0.458
Magnetic bearing coefficients,	
k_1 , N/A	13.0
k_s , N/m	6150
k_m , N/m	0.1
Gain of power amplifiers, k_Q , A/V	0.25

If we measure all coordinates represented by the vector q and differentiate all the signals, we know the whole state vector x . In this case, the

system is fully controllable and observable. Using a Riccati controller to optimize the controller with regard to the integral criterion given by equation (66), we obtain the damping represented by the real parts of the eigenvalues of the system shown in figure 14.

The weighting matrices for the results displayed by the dashed lines were chosen as

$$Q = \begin{bmatrix} Q_u & 0 \\ 0 & 0 \end{bmatrix} \quad Q_u = q_0 E \quad E \in R^{4,4} \quad q_0 = 2.5 \times 10^7 \quad (87)$$

For these results the rotor frequency chosen to design the controller was $\Omega = 150$ Hz. Figure 14 shows that the rotor is unstable up to a rotor frequency of 30 Hz, since there is negative damping associated with one of the eigenvalues below this frequency. To avoid instability, we can use an adaptive controller. This means that the controller always has to be adapted to the actual rotor frequency. The attainable results are displayed in figure 14 by the solid lines.

Control of an Elastic Rotor

A rotor consisting of an elastic shaft with a rigid body at the top supported by ball bearings was investigated (fig. 15). The shaft diameter varies with axial coordinate z ; the cross section of the shaft is constant by sectors. To improve the dynamic behavior of the rotor system, a magnetic bearing was used (fig. 15).

The essential values of most design parameters are given in table III.

TABLE III. - DESIGN PARAMETERS OF ELASTIC ROTOR SYSTEM
[See fig. 14.]

Coordinates, m	
L_0	0.0425
L_u	0.2565
L_m	0.5
s	0.0652
Moment of inertia of rigid body at end, kgm^2	
Transverse, I_{Ry}	0.0986
Polar, I_{Rz}	0.131
Mass of rigid body, m_R , kg	14.42
Bearing stiffness, N/m	
c_u	2.0×10^7
c_o	1.0×10^8
Young's modulus, E , N/m^2	2.06×10^{11}
Mass density, ρ , kg/m^3	7.85×10^3

The equation of motion can be achieved by using the theory given in the section Modeling of Actively Controlled Rotor Systems.

In the first step, the mode shape functions have to be determined. The determination of these functions is carried out separately; for example, by use of cubic spline functions, Hermite polynomials, finite elements, or experiments. The results of this determination are shown in figures 16 and 17. Figure 16 displays the eigenfrequencies with respect to rotor speed, up to the fourth order. Note that all the curves split into one forward and one backward vibration mode.

Because only the forward vibration modes can be excited by imbalances (in most cases, the dominant excitation in rotating machinery), these modes must be considered relative to the rotor speed. For this reason, the runup line ($\omega = \Omega$) is plotted in figure 16. Each intersection between the runup line and a curve of the forward eigenfrequency signifies a critical speed of the rotor. In the plot shown, two critical speeds can be recognized: $\omega_1 = 12$ Hz and $\omega_2 = 330$ Hz. In order to see the effect of the chosen actuator or sensor location on the controllability and observability of the system, the mode shapes, up to the third order for three different rotor frequencies ($\Omega = 0, 150,$ and 300 Hz), are plotted in figure 17. The actuator location is marked by M. The mode shapes and their frequencies are obviously functions of the rotor speed (gyroscopic influence). A close look shows that the controllability of the third forward and the third backward modes at $\Omega = 150$ Hz and the third backward mode at $\Omega = 300$ Hz is tending to zero; this is evidenced by the small amplitude at location M. If these modes are to be influenced effectively, the actuator location must be changed. The results attainable by state and output feedback control will be discussed in the following section.

State feedback control (Riccati controller). - The control design is based on the quadratic integral criterion shown in equation (65):

$$J = \frac{1}{2} \int_0^{\infty} (x^T Q x + u^T R u) dt \rightarrow \min \quad (88)$$

This leads to

$$J_{\text{opt}} = \frac{1}{2} x_0^T P x_0$$

where P is the solution of the algebraic Riccati equation

$$A^T P + P A - P B R^{-1} B^T P + Q = 0 \quad (89)$$

which, in connection with the criterion of equation (88), always supplies an optimal controller (gain matrix K)

$$u = -Kx \quad K = R^{-1} B^T P \quad (90)$$

A significant amount of software is already available to solve the algebraic Riccati equation.

With the vector of generalized coordinates

$$y = [y_u^T, y_v^T]^T \quad (91)$$

and the state vector

$$x = [y^T, \dot{y}^T] \quad (92)$$

the weighting matrices are chosen as

$$Q = \begin{bmatrix} 0 & 0 & 0 & 0 \\ 0 & 0 & 0 & 0 \\ 0 & 0 & Q_U & 0 \\ 0 & 0 & 0 & Q_V \end{bmatrix} \quad \text{and} \quad R = E \quad (93)$$

Only the velocities are taken into account. If we take

$$Q_U = Q_V = \text{diag}\{1.4 \times 10^7, 9 \times 10^6, 6 \times 10^6\} \quad (94)$$

we obtain, for a rotor frequency of 150 Hz, the gain matrix

$$K^T = \begin{bmatrix} -0.43 \times 10^4 & -0.81 \times 10^4 \\ -0.35 \times 10^5 & 0.29 \times 10^6 \\ 0.40 \times 10^6 & 0.27 \times 10^6 \\ \hline 0.81 \times 10^4 & -0.43 \times 10^4 \\ -0.29 \times 10^6 & -0.35 \times 10^5 \\ -0.27 \times 10^6 & 0.40 \times 10^6 \\ \hline 0.28 \times 10^4 & 0.43 \times 10^3 \\ 0.33 \times 10^4 & 0.28 \times 10^3 \\ 0.84 \times 10^3 & -0.93 \times 10^2 \\ \hline -0.42 \times 10^3 & 0.28 \times 10^4 \\ -0.28 \times 10^3 & 0.33 \times 10^4 \\ 0.93 \times 10^2 & 0.84 \times 10^3 \end{bmatrix} = \begin{bmatrix} k_1 & k_3 \\ -k_3 & k_1 \\ \hline k_5 & k_7 \\ -k_7 & k_5 \end{bmatrix} \quad (95)$$

Because the rotor is symmetric, the gain matrix can be represented

$$K = \begin{bmatrix} k_1 & -k_3 & k_5 & -k_7 \\ k_3 & k_1 & k_7 & k_5 \end{bmatrix} \quad (96)$$

It is striking that the gain matrix applies not only to $-(k_5)$, but also to artificial gyroscopic (k_7) and restraint (k_1) forces as well as to nonconservative forces (k_3). The damping equivalents with respect to rotor frequency are plotted in figure 18.

In this figure one damping curve (dashed line) is negative (the corresponding vibration mode is unstable!). This is caused by spillover effects.

To design the controller, only three mode shapes have to be taken into account; however for the model to simulate the system equations, four mode shapes were considered. Note that the design criterion guarantees asymptotic stability only for the model that was the basis for designing the controller. Figure 18 also shows that one of the damping curves approaches zero near $\Omega = 350$ Hz. This lack of damping is due to the controllability condition of this mode shape at this rotor frequency (fig. 17). We may conclude that the state feedback controller as designed is useless. A reasonable state controller would be much more expensive, so an output feedback controller will be discussed as an alternative.

Output feedback control. - In contrast to the optimization procedure of the Riccati controller leading to an optimal controller, the structure of the output controller will be fixed at the outset. For the feedback, only directly measured state coordinates are expressed by equation (62). By taking into account this measuring equation, the control vector can be written

$$u = -Ky = -Kcx = -(K_1 K_2) \begin{bmatrix} \bar{c}^T & 0 \\ 0 & \bar{c}^T \end{bmatrix} \begin{bmatrix} \bar{y} \\ \dot{\bar{y}} \end{bmatrix} \quad (97)$$

As a criterion for design of the controller, the quadratic integral criterion will be used:

$$J = \frac{1}{2} \int_0^{\infty} x^T Q x \, dt \rightarrow \min \quad (98)$$

which leads to

$$J_{opt} = \frac{1}{2} x_0^T P x_0$$

where P is a solution of $\hat{A}^T P + P \hat{A} - Q = 0$ with $\hat{A} = (A - BKC)$.

The optimization can be carried out with a presupposed starting matrix K_0 only if the system is asymptotically stable. Now, by solving the Ljapunov equation (eq. (98)) and varying the gain coefficient appearing in K , the value of the criterion can be minimized. One weak point in this procedure is that an initial state vector x_0 is necessary. On the other hand, the procedure can be used for a higher valuation of a special mode shape (here, e.g., the first forward mode). This means that for x_0 , the eigenvector (mode shape) with respect to this vibration mode has to be determined.

To reduce the calculation expense, we can take advantage of the special structure of K (properties of symmetry)

$$K = (K_1 K_2) = \begin{bmatrix} k_1 & -k_3 & k_5 & -k_7 \\ k_3 & k_1 & k_7 & k_5 \end{bmatrix} \quad (99)$$

When compared to the results of the Riccati controller (eq. (95)), equation (99) shows that to achieve an optimal controller, forces that act like gyroscopic forces (k_7) and nonconservative forces (k_3) have to be added.

The gain coefficients obtained when using the same weighting matrices as given by equation (93) are

$$\left. \begin{aligned} k_1 &= -1.9 \times 10^5 \\ k_3 &= 2.3 \times 10^4 \\ k_5 &= 2.4 \times 10^3 \\ k_7 &= -9.0 \times 10^2 \end{aligned} \right\} \quad (100)$$

The results, plotted in figure 19, show that in contrast to the Riccati controller, the system is stable at all rotor frequencies. The slight damping of one of the vibration modes is still there, but this problem can be solved by changing the actuator location (changing the controllability).

CONCLUDING REMARKS

Active vibration control of rotating machinery is being given more and more attention by research institutes as well as by industry. The purpose of this report is to present the problems confronted when applying active control techniques to rotating machinery dynamics. The success or failure of active measures is determined by the availability of appropriate actuators; by modeling of the entire system, including all active elements involved; by positioning of actuators and sensors; and by the control concept used. All of these topics have been addressed, and their special problems have been discussed in detail in this report. A survey of existing actuators as well as those that are still in the design stage is included.

A very efficient method - called "hybrid multibody systems" - was described and used to analyze rotor systems consisting of rigid and elastic subsystems. This method allows a modular construction of the system, which is very easy to handle on a computer and is both systematic and clear. Furthermore, control aspects can be adequately considered (e.g., simple system adaptations, with respect to actuator and sensor locations, or optimization strategies for designing the controller).

Such important aspects as controllability, observability, and spillover were discussed. A method of checking on these system properties was outlined, and examples were displayed. Then, the most frequently used control concepts were introduced and their strengths and weaknesses pointed out. Real applications served as examples to demonstrate how to design an optimal controller. These examples indicate a possibility for improving rotating machinery by applying active vibration control.

APPENDIX - SYMBOLS

A	system matrix
A	moment of inertia
A*	characteristic membrane area
a ^S	vector of acceleration of center of mass
B	control matrix
b	thickness of disk
b _v	gain coefficient of servo valve
C	measurement matrix
C	moment of inertia
C _M	membrane stiffness
C _R	constant considering fluid flow losses
C _T	constant considering oil inertia
C _V	constant considering fluid flow losses
c	stiffness coefficient
c _v	stiffness of servo valve
D	damping matrix
d	shaft diameter
d _v	damping of servo valve
E	identity matrix
F	vector of control forces
FV(S), F2(S)	transfer functions (Laplace domain)
f	number of degrees of freedom
f ^e	external force vector acting on a body
df ^e	external force vector acting on a mass element or disk element
f _v	generalized coordinate of servo valve
G	gyroscopic matrix

G	weight
h	vector of generalized forces
I	tensor of moments of inertia of a body
dI	tensor of moments of inertia of a mass element
i	index; or magnetic bearing current
J	performance index
J _R	Jacobian matrix of rotation; $\partial\omega/\partial\dot{q}$
J _T	Jacobian matrix of translation; $\partial\dot{r}/\partial\dot{q}$
j	index
K	stiffness matrix; or gain matrix
K _{pq} , K _v	servo valve constants
k	gain factor; or number of substructures
L	length
M	mass matrix
M ^e	external torque vector acting on a body
dM ^e	external torque vector acting on a mass element
m	mass
dm	mass element
m _v	mass influence of servo valve
N	nonconservative matrix
n	order of state space representation; or index
O	zero matrix
o	index
P	matrix for forces proportional to velocities; or solution of algebraic Riccati equation; or solution of Ljapunov equation
P	pressure
Q	matrix for forces proportional to displacements; or weighting matrix

q	vector of generalized coordinates
R	outer membrane radius
r	inner membrane radius; or number of actuators
$r(z,t)$	position vector
s	Laplace operator; $b + j\omega$
T	oil temperature
$T(j\omega)$	transfer function
t	torque vector
t	time
U_v	control voltage to the servo valve
u	control vector
$u(z)$	vector of admissible shape functions
$u(z,t)$	distributed coordinate (displacement of rotor axis in x-direction)
$v(z)$	vector of admissible shape functions
$v(z,t)$	distributed coordinate (displacement of rotor axis in y-direction)
x	state space vector
x	displacement of rotor in x-direction
x_B	bearing displacement in x-direction
\dot{x}_0	characteristic flow velocity
y	measurement vector
y	displacement of rotor in y-direction
z	axial rotor coordinate
α	angle of rotation about x-axis
β	angle of rotation about y-axis
δ	indicates variation (here only of position); Dirac function
λ	eigenvalue

ξ_v	servo valve damping coefficient
ρ	mass density
φ	vector of rotation
$\delta\varphi$	small virtual rotation
Ω	rotor frequency
ω	vector of angular velocity
$\bar{\omega}$	skew-symmetric tensor of angular velocities
ω_v	servo valve eigenfrequency

Subscripts

A	acceleration or actuator
B	bearing
D	derivative
I	integral; or inertial
M	magnetic bearing; or measuring location
O	output controller
P	proportional
R	rotor; or rotating
S	sensor location; or state controller
x,y,z	directions of coordinates

Superscripts

e	external
s	center of mass
T	transposed

Mathematical symbols

$\mathbf{a} \in \mathbb{R}^n$	vector \mathbf{a} of dimension $n \times 1$
$\mathbf{A} \in \mathbb{R}^{m,n}$	matrix \mathbf{A} of dimension $m \times n$

- () derivative with respect to time; $\partial/\partial t$
- \int
(S) integral over entire system
- δ variation with respect to displacements or rotation (no time variation)

REFERENCES

1. Ulbrich, H.: Entwurf und Realisierung einer berührungsfreien Magnetlagerung für ein Rotorsystem. Ph.D. Thesis, TU München, 1979.
2. Ulbrich, H.; Schweitzer, G.; and Bauser, E.: A Rotor Supported Without Contact - Theory and Application. World Congress on Theory of Machines and Mechanisms, 5th, Concordia University, Montreal, 1979, Proceedings, Vol. 1, ASME, New York, 1979, pp. 181-184.
3. Ulbrich, H.; and Fürst, S.: Modeling and Active Vibration Control of Flexible Rotors. World Congress on Theory of Machines and Mechanisms, 7th, Sevilla, Spain; E. Bautista, G.K. Lomas, and A. Navarro, eds., Pergamon Press, New York, 1987, pp. 1739-1743.
4. Anton, E.; and Ulbrich, H.: Active Control of Vibrations in the Case of Asymmetrical High-Speed Rotors by Using Magnetic Bearings. J. Vib. Acoust. Stress. Reliab., vol. 107, Oct. 1985, pp. 410-415.
5. Fürst, S.; and Ulbrich, H.: An Active Support System for Rotors with Oil-Film Bearings. Presented at the 4th International Conference on Vibrations in Rotating Machinery, Sept. 13-15, 1988, Edinburgh, Scotland.
6. Bleuler, H.; and Salm, J.: Active Electromagnetic Suspension and Vibration Control of an Elastic Rotor with a Signal Processor. Presented at the 4th International Conference on Vibration in Rotating Machinery, Sept. 13-15, 1988, Edinburgh, Scotland.
7. Redmond, I.; McLean, R.F.; and Burrows, C.R.: Vibration Control of Flexible Rotors. ASME Paper 85-DET-127, Sept. 1985.
8. Burrows, C.; Sahinkaya, M.; and Clements, S.: Electromagnetic Control of Oil-Film Supported Rotors Using Sparse Measurements. Rotating Machinery Dynamics, Proceedings of the 11th Biennial ASME Conference on Vibration and Noise, Boston, MA, Sept. 1987, A. Muszynska and J.C. Simonis, eds., Vol. 1., ASME, New York, 1987, pp. 127-132.
9. Schweitzer, G.; and Ulbrich, H.: Magnetic Bearings - A Novel Type of Suspension. Second International Conference: Vibrations in Rotating Machinery, Mechanical Engineering Publications, Ltd, London, 1980, pp. 151-156.
10. Ulbrich, H.; and Anton, E.: Theory and Application of Magnetic Bearings with Integrated Displacement and Velocity Sensors. International Conference on Vibrations in Rotating Machinery, 3rd, University of York, England, 1984, Mechanical Engineering Publications, Ltd., London, 1984, pp. 543-551.
11. Ulbrich, H.: Dynamik und Regelung von Rotorsystemen. Fortschr.-Ber. VDI-2, Reihe 11, NR. 86, 1986, pp. 1-147.

12. Ulbrich, H.: Control of Flexible Rotors by Active Elements. Rotating Machinery Dynamics, Proceedings of the 11th Biennial ASME Conference on Mechanical Vibration and Noise, Boston, MA, 1987, A. Muszynska and J.C. Simonis, eds., Vol. 1, ASME, New York, 1987, pp. 191-196.
13. Nonami, K.: Vibration Control of Rotor Shaft Systems by Active Control Bearing. ASME Paper 85-DET-126, Sept. 1985.
14. Ulbrich, H.: New Test Techniques Using Magnetic Bearings. Magnetic Bearings: Proceedings of the 1st International Symposium, ETH Zurich, Switzerland, June 6-7, 1988, G. Schweitzer, ed., Springer-Verlag, 1988, pp. 281-288.
15. Ulbrich, H.; and Althaus, J.: Actuator Design for Rotor Control. Machinery Dynamics - Applications and Vibration Control Problems. DE-Vol. 18-2, T.S. Sankar, et al., eds. ASME, 1989.
16. Timoshenko, S.; and Woinowsky-Krieger, S.: Theory of Plates and Shells, Second ed., McGraw-Hill Book Co., 1959.
17. Bremer, H.: Dynamik und Regelung Mechanischer Systeme. Teubner Verlag, Stuttgart, 1988.
18. Müller, P.C.; and Schliehler, W.O.: Lineare Schwingungen. Akademische Verlagsgesellschaft, Wiesbaden, 1976.
19. Lückel, J.; and Müller, P.C.: Analyse von Steuerbarkeits-, Beobachtbarkeits und Störbarkeitsstrukturen linearer, zeitinvarianter Systeme, Regelungstechnik, bd. 23, 1975, s 163-171.
20. Salm, J., and Schweitzer, G.: Modelling and Control of a Flexible Rotor with Magnetic Bearings, International Conference on Vibrations in Rotating Machinery, 3rd, University of York, England, 1984, Mechanical Engineering Publications, Ltd., London, 1984, pp. 553-561.
21. Ackermann, J.: Entwurf durch Polvorgabe Regelungstechnik, Heft 6, 1977, S. 173-179 und s. 209-215.
22. Salm, J.; and Larssonneur, R.: Modellbildung und aktive Dämpfung eines Elastischen Rotors." Z. Angew. Math. Mech., bd. 4, 1985, s. 96-98.

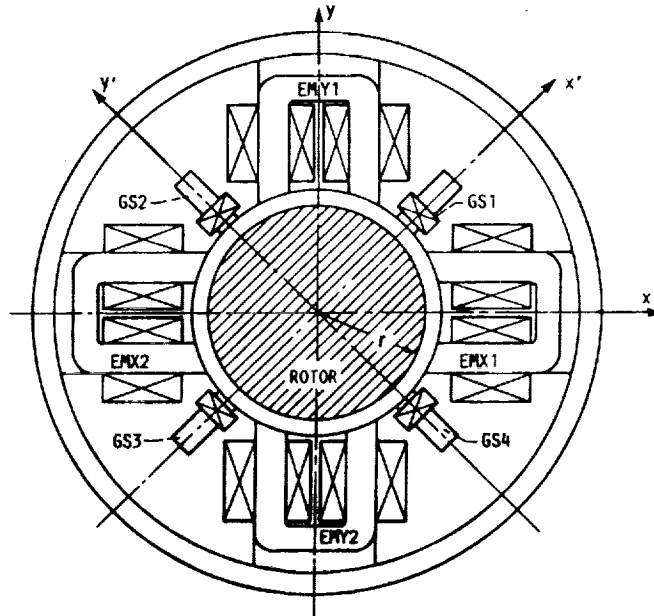


FIGURE 1. - SCHEMATIC OF A MAGNETIC BEARING WITH INTEGRATED SENSORS: EMX1, EMX2, EMY1, AND EMY2 ARE ELECTROMAGNETS; GS1 TO GS4 ARE SENSORS.

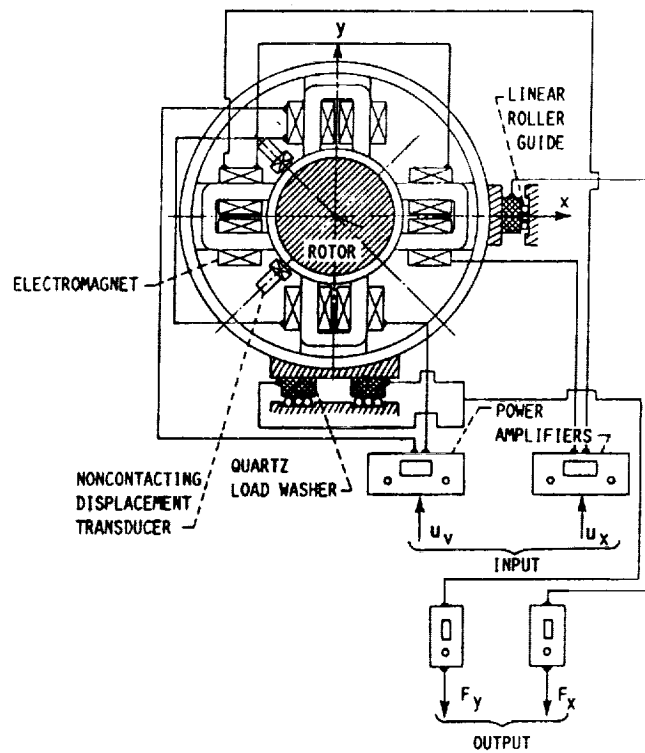


FIGURE 2. - SCHEMATIC OF MAGNETIC BEARING INCLUDING SENSOR AND ELECTRONIC DEVICES; F_x AND F_y ARE MAGNETIC BEARING FORCES; u_x AND u_y ARE VOLTAGE INPUTS TO POWER AMPLIFIERS.

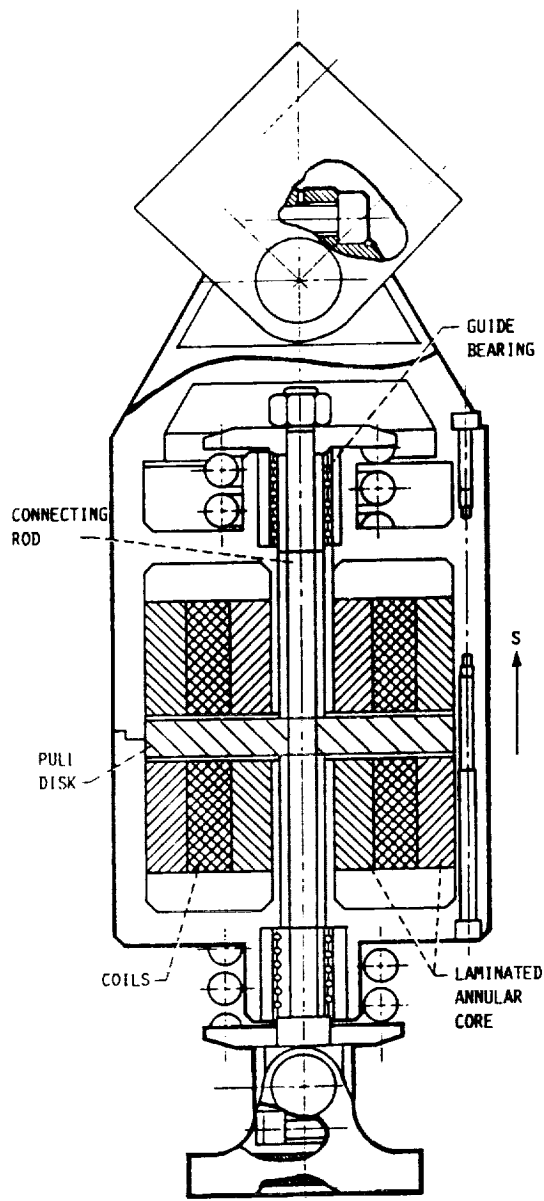
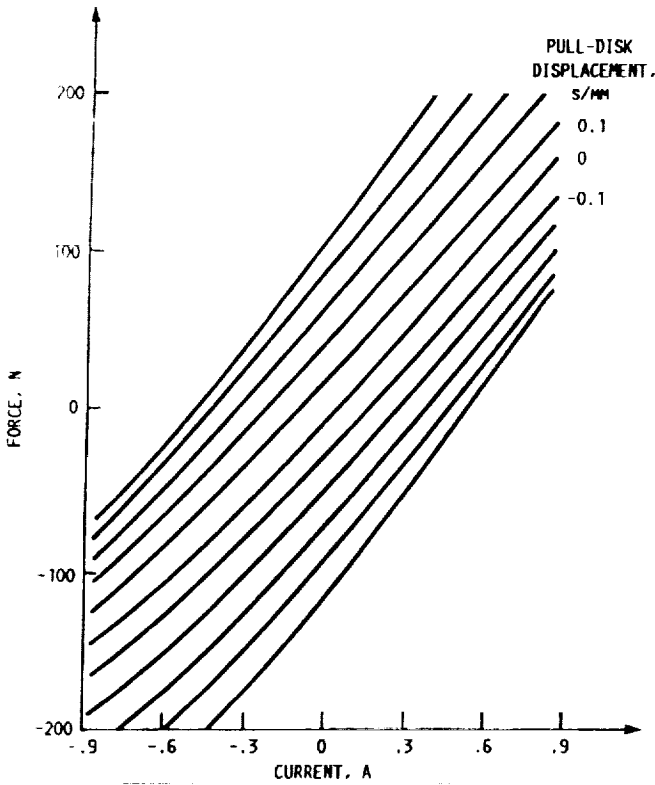
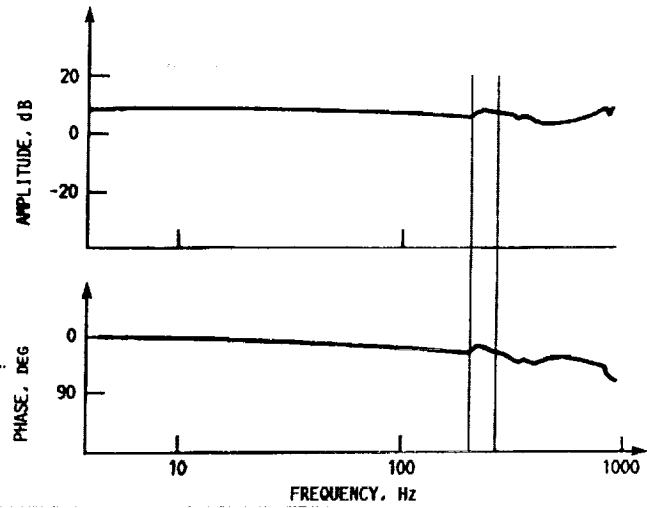


FIGURE 3. - ELECTROMAGNETIC ACTUATOR.



(a) TRANSFER CHARACTERISTIC: $k_s = 1.75 \times 10^5$ N/m;
 $k_i = 166$ N/A.



(b) FREQUENCY CHARACTERISTIC: CUTOFF FREQUENCY $f_c = 300$ Hz.

FIGURE 4. - ELECTROMAGNETIC ACTUATOR CHARACTERISTICS.

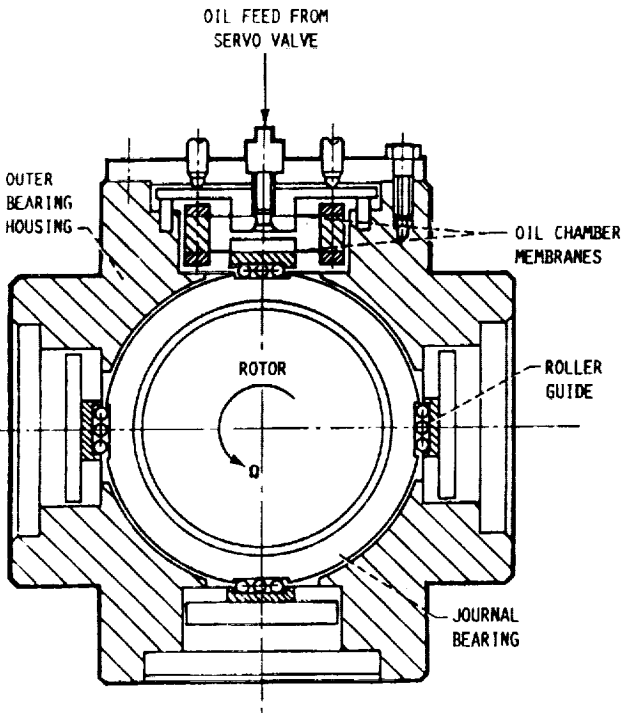


FIGURE 5. - ACTIVE CHAMBER SYSTEM.

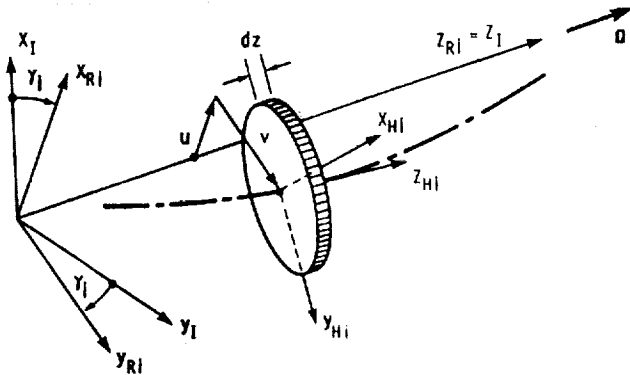


FIGURE 6. - REFERENCE FRAMES AND COORDINATES FOR THE i TH SUBSTRUCTURE: I INDICATES THE INERTIAL FRAME; R INDICATES THE ROTATING REFERENCE FRAME; AND H INDICATES THE BODY FIXED FRAME.

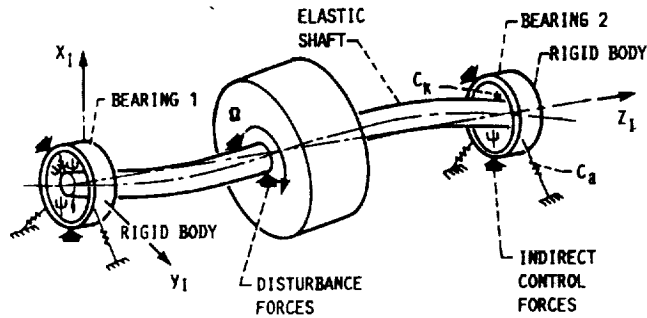


FIGURE 7. - MECHANICAL MODEL OF ROTOR SYSTEM.

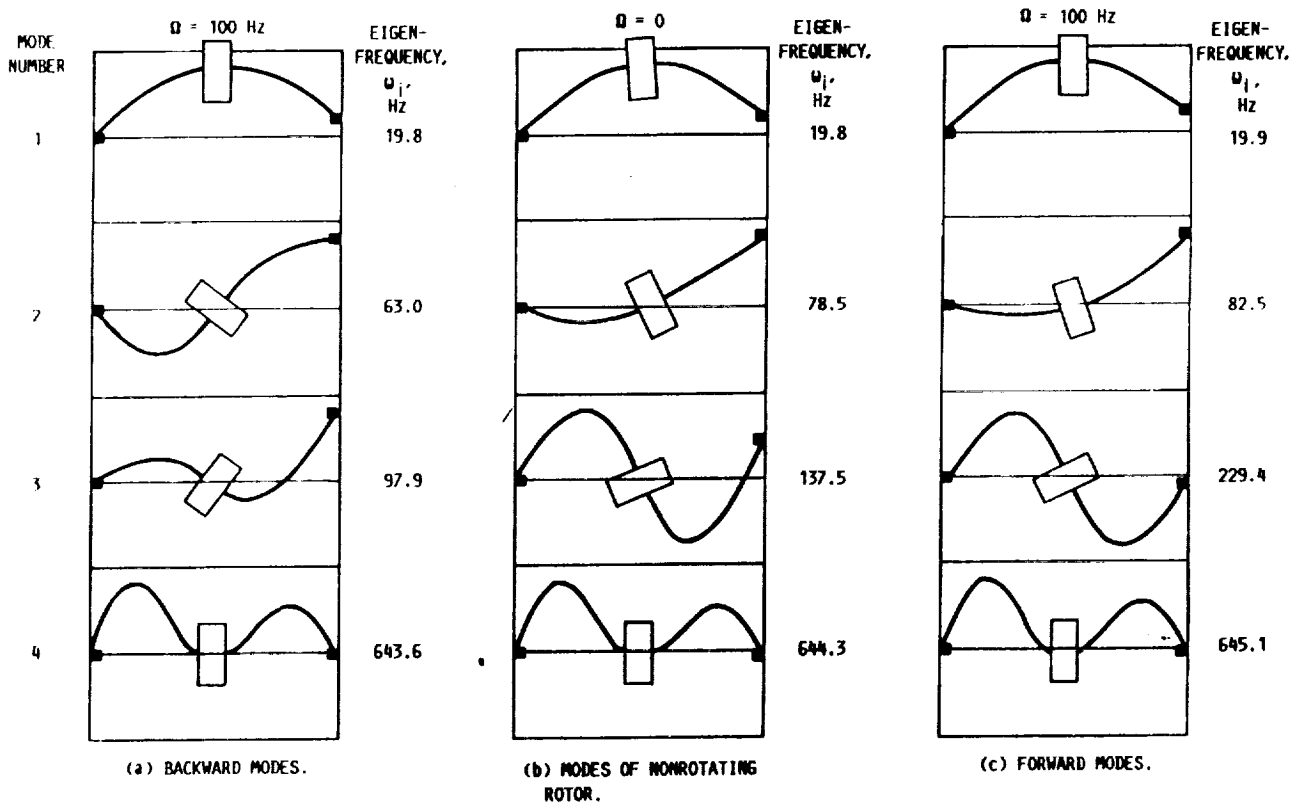
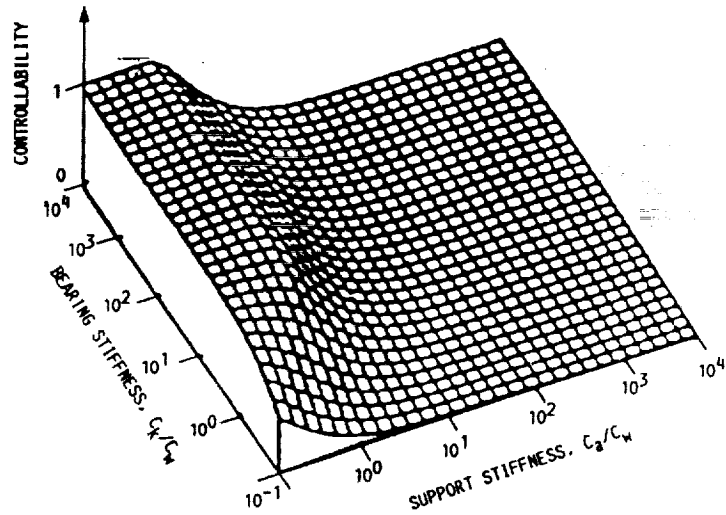
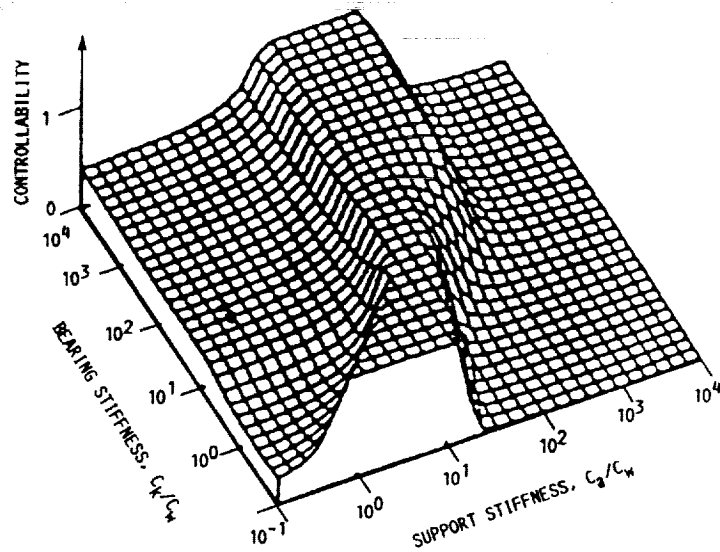


FIGURE 8. - MODE SHAPES OF THE ROTOR-BEARING SYSTEM FOR ROTOR FREQUENCIES $\Omega = 0$ AND $\Omega = 100$ Hz.



(a) FIRST FORWARD MODE.



(b) THIRD FORWARD MODE.

FIGURE 9. - CONTROLLABILITY: C_w = ROTOR STIFFNESS; C_a = BEARING SUPPORT STIFFNESS; AND C_k = BEARING STIFFNESS.

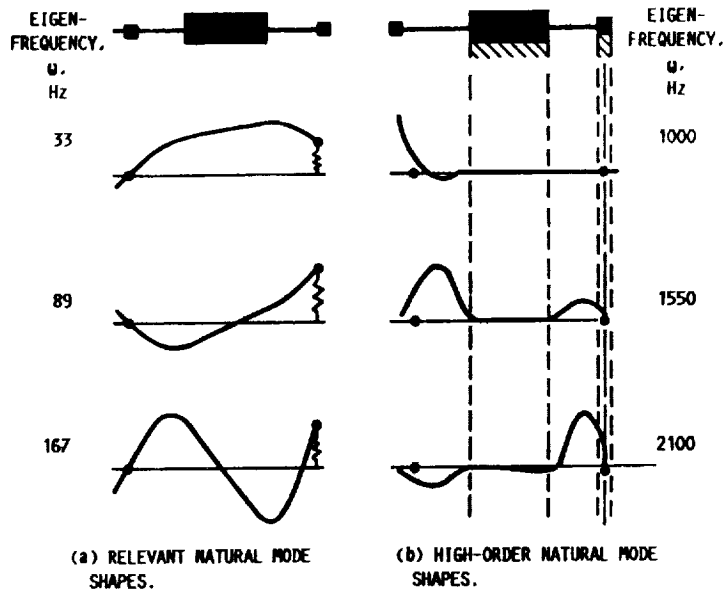


FIGURE 10. - GUIDE FOR CHOOSING ACTUATOR AND SENSOR POSITIONS FOR MINIMAL SPILLOVER (DOT SHOWS RANGE OF SUCH POSITIONS).

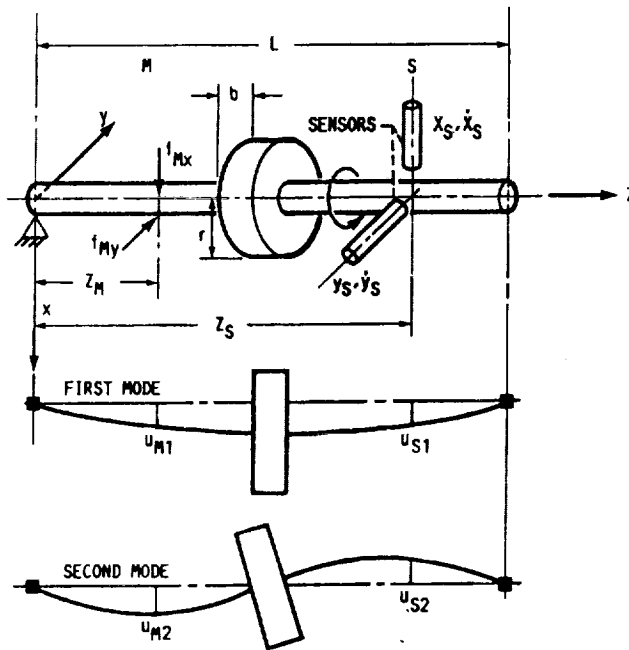


FIGURE 11. - SIMPLE ROTOR SYSTEM FOR EXPLAINING SPILLOVER EFFECTS; f_{Mx} AND f_{My} ARE ACTUATOR FORCES.

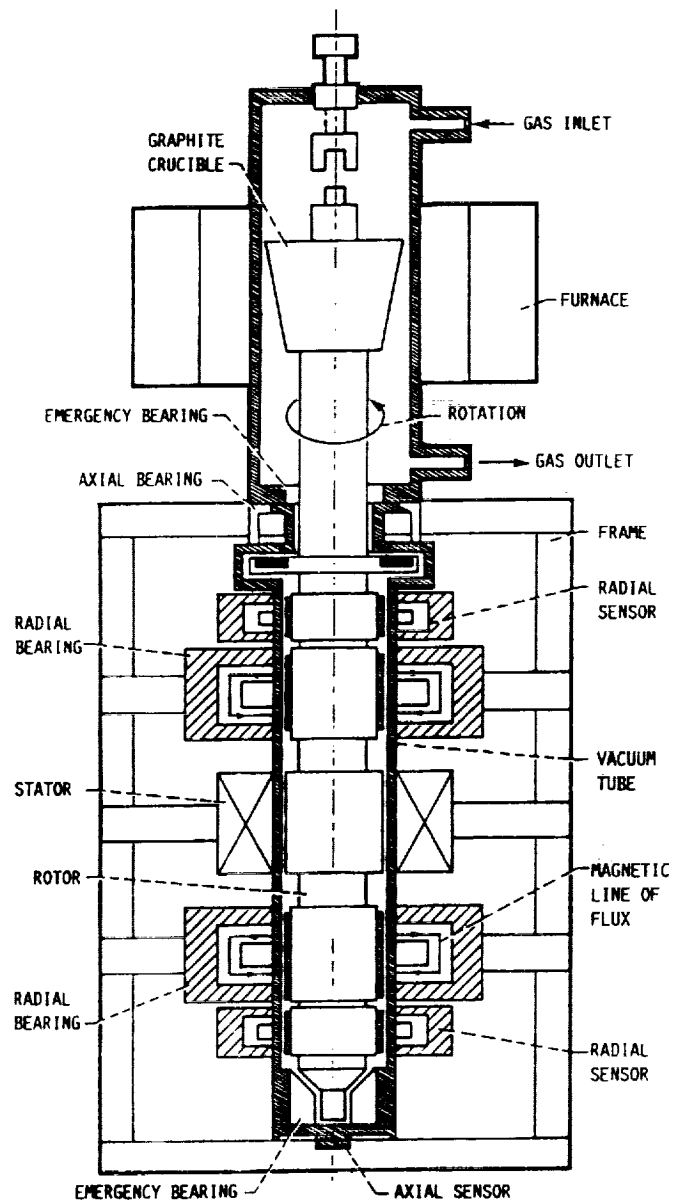


FIGURE 12. - MAGNETICALLY SUPPORTED EPITAXY CENTRIFUGE.

ORIGINAL PAGE IS
OF POOR QUALITY

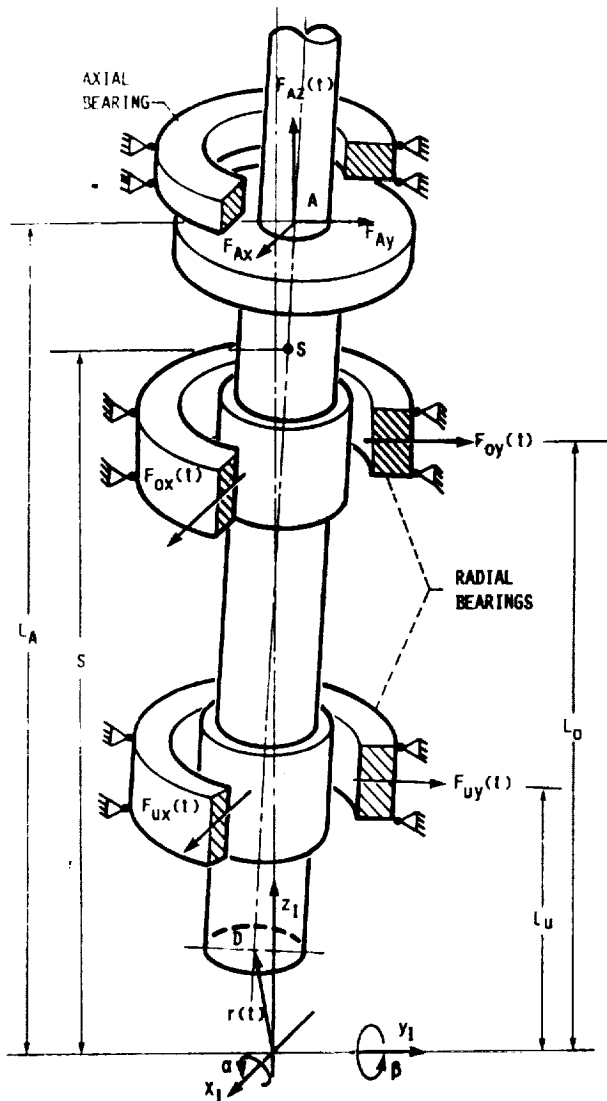


FIGURE 13. - MECHANICAL MODEL OF THE EPITAXY CENTRIFUGE.

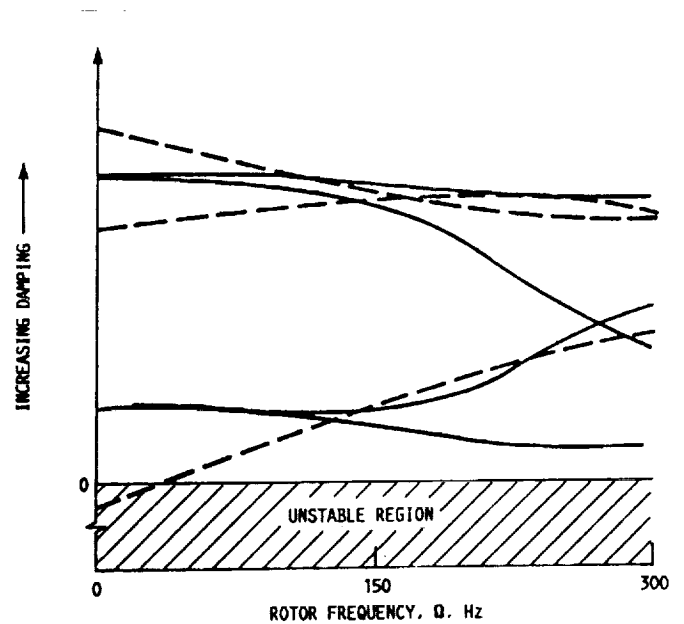


FIGURE 14. - DAMPING VALUES FOR EIGENVALUES OF EPITAXY CENTRIFUGE SYSTEM.

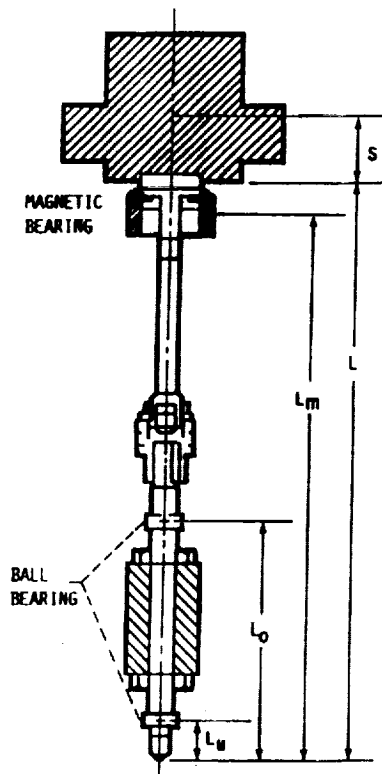


FIGURE 15. - ELASTIC ROTOR ACTIVELY INFLUENCED BY A MAGNETIC BEARING.

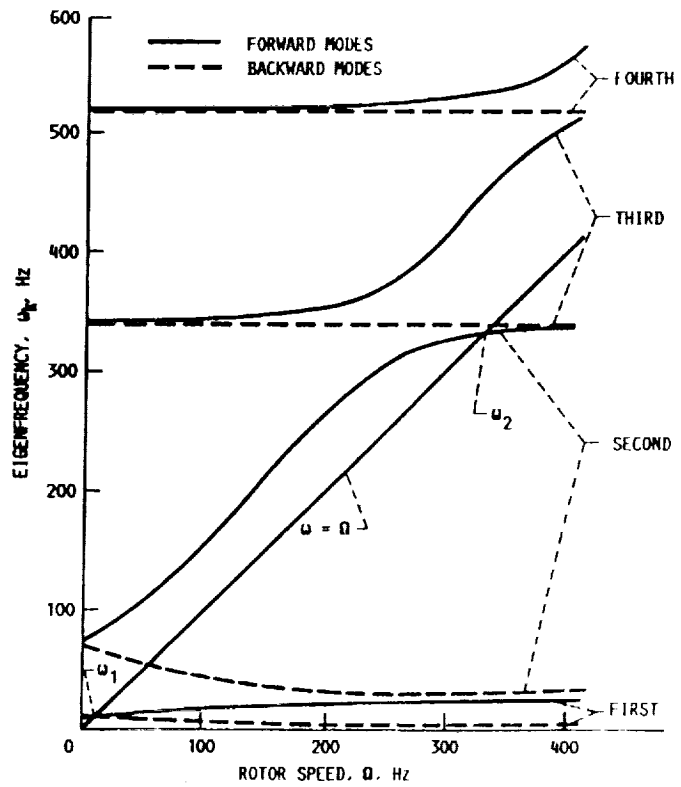


FIGURE 16. - CALCULATED PLOTS OF EIGENFREQUENCIES UP TO FOURTH ORDER OF ROTOR SHOWN IN FIGURE 15. CRITICAL SPEEDS OCCUR AT ω_1 AND ω_2 .

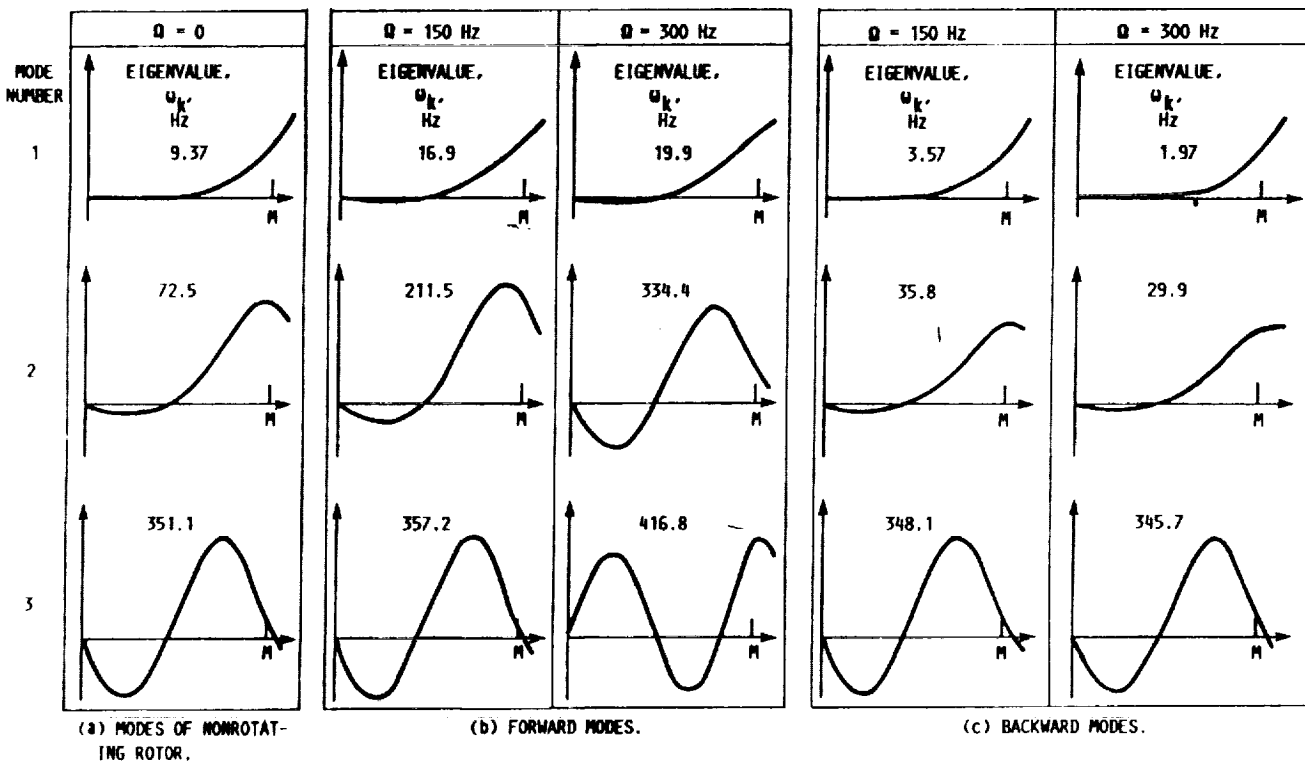


FIGURE 17. - MODE SHAPES OF THE ROTOR SHOWN IN FIGURE 15; M INDICATES ACTUATOR LOCATION.

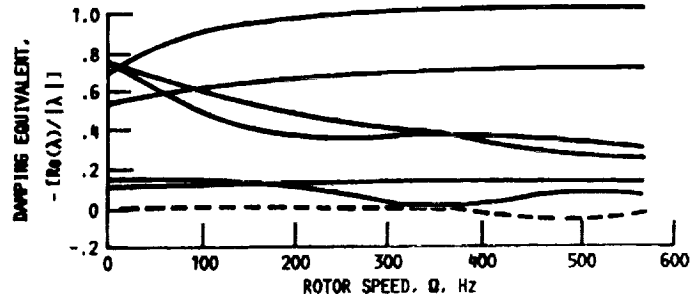


FIGURE 18. - DAMPING CURVES FOR STATE FEEDBACK CONTROL.

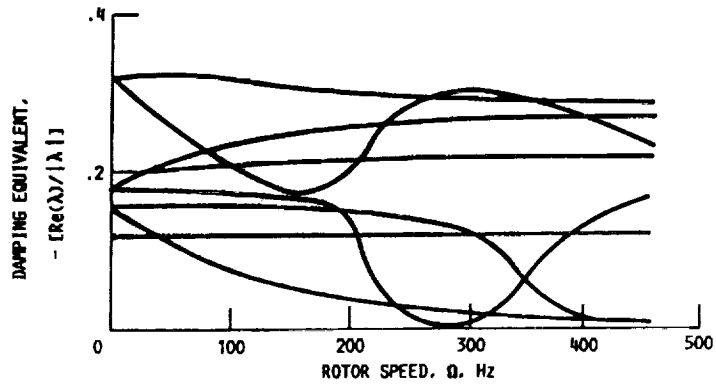


FIGURE 19. - DAMPING CURVES FOR OUTPUT FEEDBACK CONTROL.

1. Report No. NASA TM-102368		2. Government Accession No.		3. Recipient's Catalog No.	
4. Title and Subtitle Elements of Active Vibration Control for Rotating Machinery				5. Report Date May 1990	
				6. Performing Organization Code	
7. Author(s) Heinz Ulbrich				8. Performing Organization Report No. E-5036	
				10. Work Unit No. 505-63-1B	
9. Performing Organization Name and Address National Aeronautics and Space Administration Lewis Research Center Cleveland, Ohio 44135-3191				11. Contract or Grant No.	
				13. Type of Report and Period Covered Technical Memorandum	
12. Sponsoring Agency Name and Address National Aeronautics and Space Administration Washington, D.C. 20546-0001				14. Sponsoring Agency Code	
15. Supplementary Notes Heinz Ulbrich, National Research Council--NASA Research Associate at Lewis Research Center. Present address: Technical University of Braunschweig Institute of Production, Automation, and Manipulation Techniques P.O. Box 3329 D-3300 Braunschweig, F.R.G.					
16. Abstract The success or failure of active vibration control is determined by the availability of suitable actuators, modeling of the entire system including all active elements, positioning of the actuators and sensors, and implementation of problem-adapted control concepts. All of these topics are outlined and their special problems are discussed in detail. Special attention is given to efficient modeling of systems, especially for considering the active elements. Finally, design methods for and the application of active vibration control on rotating machinery are demonstrated by several real applications.					
17. Key Words (Suggested by Author(s)) Control of rotors; Actuators; Sensors; Modelling of flexible rotors; Control techniques; Magnetic bearing; Hydraulic actuator				18. Distribution Statement Unclassified - Unlimited Subject Category 31	
19. Security Classif. (of this report) Unclassified		20. Security Classif. (of this page) Unclassified		21. No. of pages 48	22. Price* A03